ARTICLE IN PRESS

Available online at www.sciencedirect.com

SCIENCE DIRECT®

ELSEVIER

Life Sciences xx (2005) xxx – xxx

Life Sciences

www.elsevier.com/locate/lifescie

Effect of the difference in vehicles on gene expression in the rat liver—analysis of the control data in the Toxicogenomics Project Database

Kayoko Takashima [a], Yumiko Mizukawa [a,c], Katsumi Morishita [a], Manabu Okuyama [a], Toshihiko Kasahara [a], Naoki Toritsuka [a], Toshikazu Miyagishima [a,b], Taku Nagao [a], Tetsuro Urushidani [a,b,c,*]

[a] *Toxicogenomics Project, National Institute of Health Sciences, 1-18-1 Kamiyoga, Setagaya-Ku, Tokyo, 158-8501, Japan*
[b] *Present address of Toxicogenomics Project, National Institute of Biomedical Innovation, 7-6-8, Saito-Asagi, Ibaraki, Osaka, 567-0085, Japan*
[c] *Department of Pathophysiology, Faculty of Pharmaceutical Sciences, Doshisha Women's College of Liberal Arts, Kodo, Kyotanabe, Kyoto 610-0395, Japan*

Received 30 July 2005; accepted 1 November 2005

Abstract

The Toxicogenomics Project is a 5-year collaborative project by the Japanese government and pharmaceutical companies in 2002. Its aim is to construct a large-scale toxicology database of 150 compounds orally administered to rats. The test consists of a single administration test (3, 6, 9 and 24 h) and a repeated administration test (3, 7, 14 and 28 days), and the conventional toxicology data together with the gene expression data in liver as analyzed by using Affymetrix GeneChip are being accumulated. In the project, either methylcellulose or corn oil is employed as vehicle. We examined whether the vehicle itself affects the analysis of gene expression and found that corn oil alone affected the food consumption and biochemical parameters mainly related to lipid metabolism, and this accompanied typical changes in the gene expression. Most of the genes modulated by corn oil were related to cholesterol or fatty acid metabolism (e.g., CYP7A1, CYP8B1, 3-hydroxy-3-methylglutaryl-Coenzyme A reductase, squalene epoxidase, angiopoietin-like protein 4, fatty acid synthase, fatty acid binding proteins), suggesting that the response was physiologic to the oil intake. Many of the lipid-related genes showed circadian rhythm within a day, but the expression pattern of general clock genes (e.g., period 2, arylhydrocarbon nuclear receptor translocator-like, D site albumin promoter binding protein) were unaffected by corn oil, suggesting that the effects are specific for lipid metabolism. These results would be useful for usage of the database especially when drugs with different vehicle control are compared.

Keywords: Toxicogenomics; Vehicle control; Methylcellulose; Corn oil; Lipid metabolism; Rat; Liver

Introduction

The Toxicogenomics Project is a 5-year collaborative project by the National Institute of Health Sciences (NIHS) and 17 pharmaceutical companies in Japan which started in 2002 (Urushidani and Nagao, 2005). In April 2005, some rearrangements were made and now the project is conducted by NIHS, the National Institute of Biomedical Innovation, and 16 pharmaceutical companies. Its aim is to construct a large-scale toxicology database of transcriptome for prediction of toxicity of new chemical entities in the early stage of drug development. About 150 chemicals, mainly medicinal compounds, have been selected, and the following are examined for each. The in vivo test using rat consists of a single administration test (3, 6, 9 and 24 h with 4 dose levels including vehicle control) as well as a repeated administration test (3, 7, 14 and 28 days with 4 dose levels including vehicle control), and the data of body weight, general symptoms, histopathological examination of liver and kidney, and blood biochemistry are obtained from each animal. The gene expression in liver (and kidney in some cases) is comprehensively analyzed by using Affymetrix GeneChip. An in vitro test using rat and human hepatocytes is also carried out to accomplish the bridging between the species. By April 2005, more than 100 chemicals, covering wide medication categories, have been finished or are ongoing.

* Corresponding author. Department of Pathophysiology, Faculty of Pharmaceutical Sciences, Doshisha Women's College of Liberal Arts, Kodo, Kyotanabe, Kyoto 610-0395, Japan. Tel.: +81 0774 65 8689.
E-mail address: turushid@dwc.doshisha.ac.jp (T. Urushidani).

0024-3205/$ - see front matter © 2005 Published by Elsevier Inc.
doi:10.1016/j.lfs.2005.11.010

Along with the effects of the chemicals, a vast amount of control data is being accumulated.

The main purpose of the project is to predict toxicity in the early stage of drug development. The potential usefulness of microarray data for the estimation of toxicity of drugs makes it possible for this technology to be used in the late stage of development, i.e., application in the field of regulatory science. In this case, however, more strict and precise validation is needed in order to assure the reliability of the data. It is well known that a difference in the platform considerably effects a variation in the microarray data (Waring et al., 2004) and this is quite difficult to overcome. In our project, either methylcellulose or corn oil is employed as vehicle, according to the dispensability of the drug. It is quite possible that the difference in the vehicle control affects the analysis, as observed by multiple comparison of drug effects. In traditional toxicological study, comparison of the drug is exclusively made against its vehicle control. However, in the transcriptome database, it is usually necessary to make a comparison among various drugs by clustering or discriminant analysis. The history of this field is not old enough for collecting appropriate data regarding this issue. Our database enables us to make various comparisons among different vehicles, protocols, facilities, chip versions, etc. In this present report, we focus on the influence of vehicles on the control parameters including the gene expression profile in the rat liver as a basic study for future analysis.

Materials and methods

Animal treatment

Male Sprague-Dawley rats were purchased from Charles River Japan Inc., (Kanagawa, Japan) at 5-weeks of age. After a 7-day quarantine and acclimatization period, the animals were divided into groups of 5 animals using a computerized stratified random grouping method based on the body weight for each age. The animals were individually housed in stainless-steel cages in a room that was lighted for 12 h (7:00–19:00) daily, ventilated with an air-exchange rate of 15 times per hour, and maintained at 21–25 °C with a relative humidity of 40–70%. Each animal was allowed free access to water and pellet food (CRF-1, sterilized by radiation, Oriental Yeast Co., Japan).

According to the protocol in our project, rats in each group were orally administered with various drugs suspended or dissolved either in 0.5% methylcellulose solution or corn oil according to their dispersibility. Each drug had 4 different dose levels, including the vehicle control alone, which was exclusively analyzed in the present study. Drug treatment was performed between 9:00 and 11:30 a.m. For single-dose experiments, rats were sacrificed at 3, 6, 9, and 24 h after dosing. For repeated dose experiments, the animals were treated for 3, 7, 14 or 28 days, and they were sacrificed 24 h after the last dosing. Body weights were recorded every day while food consumption was recorded every 4 days during repeated dosing. Blood samples were collected upon sacrifice in tubes containing heparin lithium (blood biochemistry), EDTA-2K (hematology), or 1/9 vol of 3.8% citric acid (coagulation), and the following items were examined: hematology: the numbers of red blood cells, reticulocytes, white blood cells, eosinophils, monocytes, platelets, neutrophils, basophils, and lymphocytes, hemoglobin, mean red blood cell volume, mean hemoglobin contents, and mean hemoglobin concentration (Advia 120, Bayer); blood coagulation: prothorombin time, active partial prothrombin time, and fibrinogen (Sysmex CA-5000, Sysmex); and blood biochemistry: alkaline phosphatase, total cholesterol, triglyceride, phospholipid, total and direct bilirubin, glucose, blood urea nitrogen, creatinine, Na, K, Ca, Cl, inorganic phosphate, total protein, albumin, globulin/albumin ratio, aspartate aminoptansferase, alanine aminotransferase, lactate dehydrogenase, and γ-glutamyltranspeptidase, which were determined by an autoanalyzer (Hitachi 7080).

When the analysis was performed (April 2005), 65 compounds had been completed in 4 different contract research organizations. In order to eliminate the variations due to the difference in the facility, we selected a laboratory (Japan Bioassay Center, Kanagawa, Japan) where at least 7 experiments for each vehicle were completed. As 10 experiments were done with methylcellulose as the vehicle there, the latest 3 of them were excluded from the present analysis to match the numbers. Therefore, each time point consists of 35 (5 rats for 7 experiments) animals.

The experimental protocols were reviewed and approved by the Ethics Review Committee for Animal Experimentation of National Institute of Health Sciences.

Microarray analysis

After collecting the blood, the animals were euthanized by exsanguination from the abdominal aorta under ether anesthesia. An aliquot of the sample (about 30 mg) for RNA analysis was obtained from the left lateral lobe of the liver in each animal immediately after sacrifice, kept in RNA later® (Ambion, Austin, TX, USA) overnight at 4 °C, and then frozen to send to the facility in the National Institute of Health Sciences.

Total RNA was isolated using RNeasy kit by Bio Robot 3000 (Qiagen, Valencia, CA, USA). Homogenization was conducted by Mill Mixer (Qiagen) and zirconium beads. Purity of the RNA was checked by gel electrophoresis confirming the 260/280 nm ratio was between 2.0 and 2.2.

Microarray analysis was conducted on 3 out of 5 samples for each group by using GeneChip® RAE230A probe arrays (Affymetrix, Santa Clara, CA, USA), containing 15923 probe sets. The procedure was conducted basically according to the manufacturer's instructions using Superscript Choice System (Invitrogen, Carlsbad, CA, USA) and T7-$(dT)_{24}$-oligonucleotide primer (Affymetrix) for cDNA synthesis, cDNA Cleanup Module (Affymetrix) for purification, and BioArray High yield RNA Transcript Labeling Kit (Enzo Diagnostics, Farmingdale, NY, USA) for synthesis of biotin-labeled cRNA. Ten micrograms of fragmented cRNA was hybridized to a RAE230A probe array for 18 h at 45 °C at 60 rpm, after which the array was washed and stained by streptavidin-phycoerythrin using

Fluidics Station 400 (Affymetrix) and scanned by Gene Array Scanner (Affymetrix).

In the middle of the project (2004), Affymetrix released ver. 2.0 GeneChip and we switched from RAE230A to 230.2. Two out of seven experiments were performed using the new chips, and they were excluded from the present analysis in order to maintain consistency. Therefore, each time point consisted of 15 measures (3 rats for 5 experiments) in the case of gene expression analysis.

The digital image files were processed by Affymetrix Microarray Suite version 5.0 and the intensities were normalized for each chip by setting the mean intensity to 500 (per chip normalization). The results of the DNA microarray analysis are available upon request (e-mail to turushid@dwc.doshisha.ac.jp).

Statistical analysis

For conventional toxicological parameters, it is common that many unimportant changes with statistical significance are observed because of the large numbers of measurements. In the present study, more than 40 parameters were measured for 8 time points (3, 6, 9, 24 h for single and 3, 7, 14, 28 days for repeated administration). For comparison between methylcellulose and corn oil, we applied Student's t-test with Bonferroni's adjustment for each parameter, i.e., p value was multiplied by 8 and $p<0.01$ was considered to be statistically significant.

For gene expression data, it is problematic to use a standard t-test, because of too many comparisons, but it is also not good to use a too conservative adjustment, because of the small

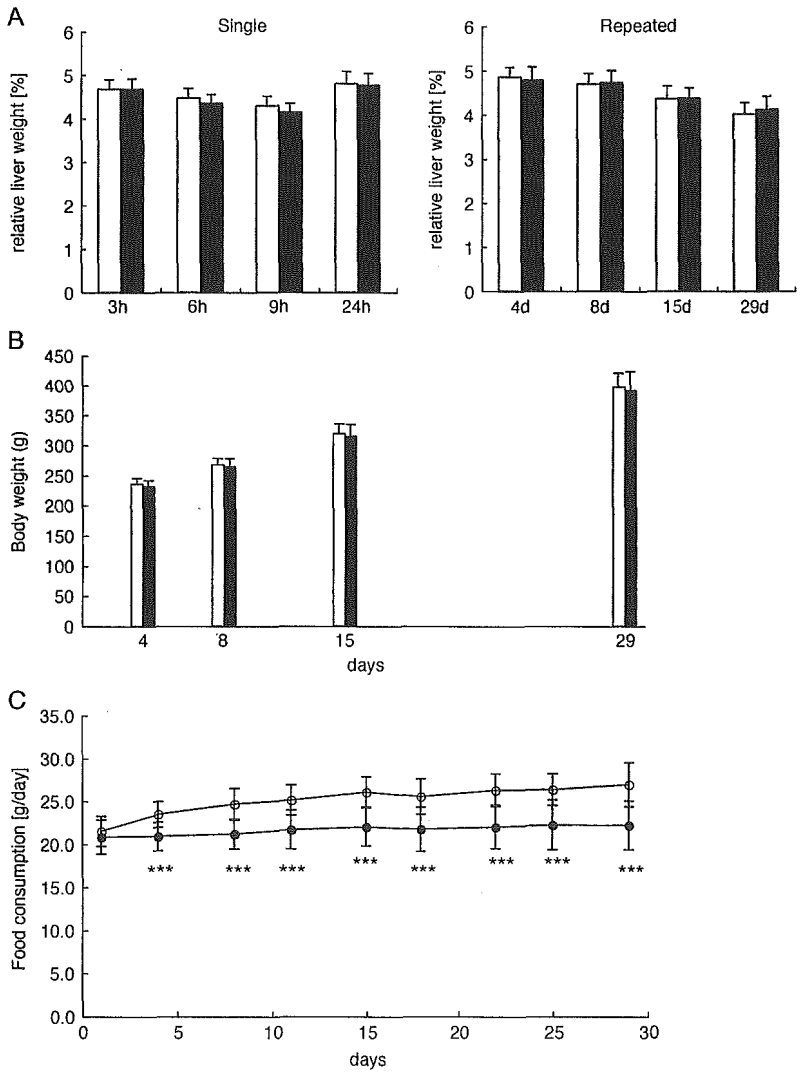

Fig. 1. Effects of different vehicles on relative liver weight, body weight, and food consumption of rats. Liver weight/body weight within 24 h after administration of vehicle and 24 h after the repeated administrations (for 3, 7, 14 and 28 days) of vehicle were measured at autopsy (A). Open and filled columns represent methylcellulose and corn oil, respectively. Body weight 24 h after the repeated administrations (for 3, 7, 14 and 28 days) of vehicle (B) and food consumption measured every 4 days and expressed as g/day (C) are plotted. Again, open and filled symbols represent methylcellulose and corn oil, respectively. Values are expressed as mean ± SD of 35 rats each for each time point. Food consumption data were obtained from rats that received either vehicle for 28 days. ***Statistically significant between methylcellulose and corn oil by Student's t-test with Bonferroni's adjustment, at $p<0.001$.

numbers of samples compared with the numbers of genes. In the present study, we considered that the β-error should be small, since our purpose was to pick up the possible vehicle effects on gene expression. Before comparison, the genes that showed less than 20 of the expression value after per chip normalization in all the samples were excluded. Genes extracted were those showing at least 1.5 fold difference between two vehicles, with $p<0.01$ (uncorrected t-test).

Results

It is common that some statistically significant but unimportant differences are observed in toxicological tests where huge numbers of parameters are measured and compared. In the present analysis of the vehicle effect, there appeared to be some differences that could not be ignored. Fig. 1A depicts the relative weight of the liver (liver weight/body weight). As is widely known, this parameter showed a clear circadian rhythm, i.e., it decreases toward the evening (9 h after dosing) and goes back in the next morning (Fig. 1A, left). In the case of rats receiving corn oil, this parameter tended to be lower than that in methylcellulose group at 6 and 9 h after dosing ($p=0.03$ and $p=0.005$, respectively, by standard t-test, but $p=0.24$ and $p=0.04$, respectively, by Bonferroni's adjustment and not significant at $p<0.01$), whereas the values returned to the same level at 24 h after administration. There was no difference in this parameter in the repeated administration, suggesting that the tendency of the decrease in the liver weight by corn oil was not accumulated during repeated dosing (Fig. 1A, right). Fig. 1 shows the body weight change (B)

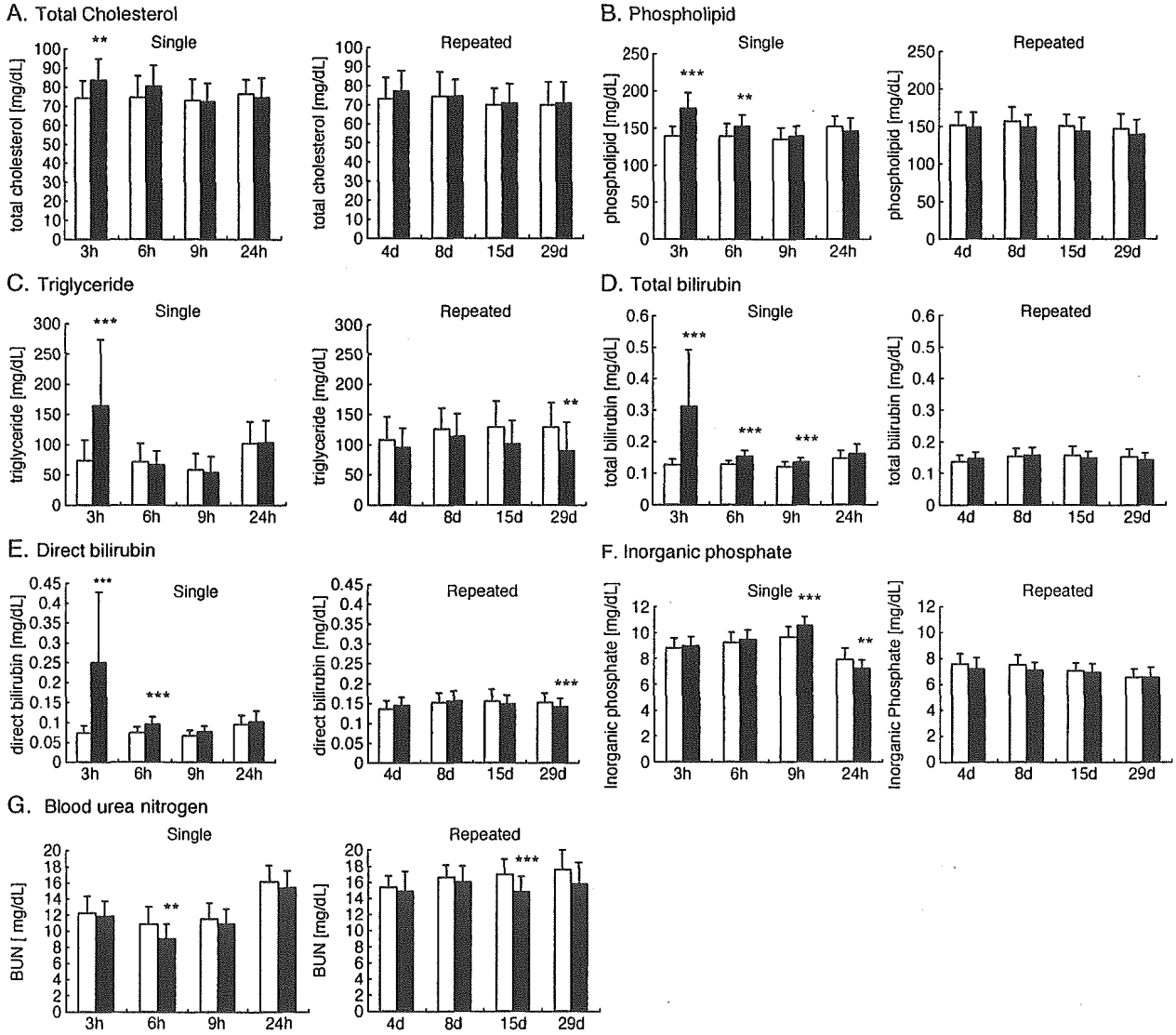

Fig. 2. Blood biochemical parameters in rats receiving methylcellulose or corn oil. Total cholesterol (A), triglyceride (B), phospholipid (C), total bilirubin (D) and direct bilirubin (E), inorganic phosphate (F), and blood urea nitrogen (G) showed a significant difference between methylcellulose (open columns) and corn oil (closed columns) among 36 parameters. Values are expressed as mean±SD of 35 rats for each time point. Statistically significant between methylcellulose and corn oil by Student's t-test with Bonferroni's adjustment, at $^{**}p<0.01$, $^{***}p<0.001$.

Table 1
List of genes showing at least a 1.5 fold difference with $p<0.01$ (uncorrected t-test) between methylcellulose and corn oil at any point during 24 h after single dose or at 29th day of repeated dose

Probe set ID	Gene title	Gene symbol	3 h	6 h	9 h	24 h	29 d
1367707_at	fatty acid synthase	Fasn	0.995	1.738	1.300	0.722	0.596
1367708_a_at	fatty acid synthase	Fasn	0.982	1.500	1.182	0.826	0.678
1367729_at	ornithine aminotransferase	Oat	1.223	1.140	1.066	0.792	0.653
1367836_at	carnitine palmitoyltransferase 1, liver	Cpt1a	1.325	1.483	1.535	0.888	1.305
1367854_at	ATP citrate lyase	Acly	1.081	1.741	1.295	0.882	0.760
1367946_at	PDZ and LIM domain 1 (elfin)	Pdlim1	0.762	0.661	0.777	0.914	0.977
1367959_a_at	sodium channel, voltage-gated, type I, beta polypeptide	Scn1b	1.042	1.013	1.567	1.613	1.278
1368035_a_at	protein tyrosine phosphatase, receptor type, F	Ptprf	0.935	1.009	0.649	0.920	0.985
1368160_at	insulin-like growth factor binding protein 1	Igfbp1	1.239	0.485	1.238	0.631	1.143
1368272_at	glutamate oxaloacetate transaminase 1	Got1	1.623	0.989	0.965	0.687	0.813
1368275_at	sterol-C4-methyl oxidase-like	Sc4mol	0.902	1.224	1.552	0.929	0.857
1368428_at	X-prolyl aminopeptidase (aminopeptidase P) 2, membrane-bound	Xpnpep2	0.839	0.896	0.668	0.783	0.916
1368435_at	cytochrome P450, family 8, subfamily b, polypeptide 1	Cyp8b1	1.534	1.860	1.570	0.711	0.798
1368458_at	cytochrome P450, family 7, subfamily a, polypeptide 1	Cyp7a1,	0.471	1.768	1.310	0.586	0.607
1368569_at	aldo-keto reductase family 1, member B7	Akr1b7	0.197	0.971	0.190	2.782	5.398
1369073_at	nuclear receptor subfamily 1, group H, member	Nr1h4	1.165	1.594	1.190	0.903	1.047
1369195_at	fatty acid binding protein 2, intestinal	Fabp2	0.901	1.135	1.022	1.753	1.753
1369238_at	inhibin beta E	Inhbe	1.441	1.553	1.067	1.034	0.934
1369415_at	basic helix-loop-helix domain containing, class B2	Bhlhb2	1.019	1.814	1.449	0.983	0.862
1369440_at	ATP-binding cassette, sub-family G (WHITE), member 8	Abcg8	0.676	0.538	0.701	0.893	1.440
1369493_at	prolactin receptor	Prlr	0.609	0.958	0.717	1.147	1.975
1369663_at	epoxide hydrolase 2, cytoplasmic	Ephx2	1.073	1.346	1.616	1.196	1.844
1369674_at	purinergic receptor P2X, ligand-gated ion channel, 5	P2rx5	1.930	0.838	0.893	0.811	1.065
1369790_at	tyrosine aminotransferase	Tat	0.771	0.624	1.094	0.735	0.837
1369864_a_at	serine dehydratase	Sds	1.509	0.429	0.872	0.482	0.538
1370024_at	Fatty acid binding protein 7, brain	Fabp7	1.044	0.964	1.057	1.312	1.524
1370336_at	pregnancy-induced growth inhibitor	Okl38	0.615	0.694	0.735	1.091	1.139
1370355_at	stearoyl-Coenzyme A desaturase 1	Scd1	1.206	1.197	1.065	0.904	0.604
1370427_at	platelet derived growth factor, alpha	Pdgfa	1.066	0.912	1.155	0.559	1.097
1371127_at	bone morphogenetic protein 1 (procollagen C-proetinase)	RGD:620739	0.815	1.175	0.950	0.991	1.557
1371234_at	fibrinogen, B beta polypeptide	Fgb	1.165	0.990	0.896	0.894	0.639
1371279_at	histone 2a /// similar to Histone H2A.1	RGD:621437	1.093	0.910	0.798	0.604	0.843
1371595_at	Transcribed locus, weakly similar to XP346694.1 Rattus norvegicus LOC360381 gene	---	0.738	0.639	0.607	0.824	0.938
1371754_at	solute carrier family 25 (mitochondrial carrier, phosphate carrier), member 25	Slc25a25	0.939	0.891	1.187	0.912	0.660
1372188_at	Endothelial cell growth factor 1 (platelet-derived) (predicted)	---	1.043	1.548	1.053	1.187	1.051
1372276_at	Transcribed locus	---	0.941	1.673	1.209	1.340	1.714
1372536_at	Chaperone, ABC1 activity of bc1 complex like (S. pombe) (predicted)	---	0.953	0.973	0.659	0.904	1.082
1374265_at	Similar to arylacetamide deacetylase (esterase) (predicted)	---	0.964	1.221	1.511	0.872	0.853
1374932_at	---	---	0.818	1.705	0.745	1.055	0.897
1375367_at	PDZ and LIM domain 2	Pdlim2	1.283	1.623	1.002	0.870	0.896
1375422_at	---	---	1.094	0.936	1.875	1.039	1.025
1375552_at	---	---	0.889	1.176	0.927	0.932	1.584

Data are expressed as the ratio of gene expression (methylcellulose=1) and columns with significant change are shaded ($N=15$ for each group).

together with food consumption (C). Although both methylcellulose and corn oil groups got weight in the same rate during repeated dosing, food consumption in the corn oil group was significantly lower than that in methylcellulose group by about 15% throughout the period of repeated administration.

Among the hematological and blood biochemical parameters, mean corpuscular hemoglobin concentration (at 15th day), platelets (at 9 h), monocytes (at 3 h), prothrombin time (at 29th day), activated partial thromboplastin time (at 24 h), fibrinogen (at 3 h), chloride (at 3 h) showed statistically significant differences between corn oil and methylcellurose. However, these changes were not considered to be important, since their changes were small and no changes in related parameters were associated. On the other hand, total cholesterol, phospholipids, triglyceride, and bilirubin (both total and direct) were found to be significantly different between vehicle controls (Fig. 2A–E). All of them showed significantly higher values in the corn oil group at 3 h after dosing, and the differences abated or disappeared at 6 h or later. In the repeated administration, the corn oil group showed rather lower values of triglyceride, total and direct bilirubin. Inorganic phosphate showed a significantly higher value in corn oil at 9 h and went down to a lower value than methylcellulose (Fig. 2F). Blood urea nitrogen (Fig. 2G) showed a lower value in corn oil at 6 h and 15th day.

Scatter plots of gene expression between vehicle controls at each time point revealed that most of the genes distributed within a 2-fold range of their 45° line, meaning that few

Table 1 (*continued*)

Probe set ID	Gene title	Gene symbol	3 h	6 h	9 h	24 h	29 d
1375619_at	---	---	1.171	0.667	0.789	0.971	0.756
1375796_at	interferon gamma induced GTPase (predicted)	Igtp_predicted	1.005	0.883	1.021	1.787	0.847
1376313_at	two pore segment channel 2 (predicted)	RGD:1311779	1.040	0.800	0.871	0.991	1.956
1376657_at	immunoglobulin superfamily, member 4A (predicted)	Igsf4a_predicted	1.060	1.749	1.510	0.868	1.022
1376704_a_at	necdin-like 2 (predicted)	Ndnl2_predicted	1.048	0.886	1.061	0.995	0.660
1376892_at	---	---	1.109	0.949	0.854	0.654	0.953
1376958_at	Similar to serine (or cysteine) proteinase inhibitor, clade B, member 9	---	0.456	0.824	1.105	1.206	1.039
1377361_at	---	---	1.004	0.667	0.794	0.890	1.020
1379252_at	Immunoglobulin superfamily, member 4A (predicted)	---	1.083	1.505	1.476	0.861	0.970
1383075_at	cyclin D1	Ccnd1	0.636	0.693	0.945	1.029	1.211
1384178_at	Leucine rich repeat containing 4B (predicted)	---	0.906	0.656	0.890	0.802	0.884
1384288_at	Transcribed locus	---	1.119	0.596	1.136	0.835	1.054
1386041_a_at	Kruppel-like factor	Klf2	1.986	0.850	1.345	1.004	1.053
1386789_at	---	---	1.305	0.611	1.196	1.134	1.003
1387017_at	squalene epoxidase	Sqle	0.927	1.279	1.832	1.058	0.980
1387022_at	aldehyde dehydrogenase family 1, member A1	Aldh1a1	0.769	1.099	0.913	1.039	1.804
1387123_at	cytochrome P450, family 17, subfamily a, polypeptide 1	Cyp17a1	1.003	0.982	1.106	1.309	1.613
1387183_at	carnitine O-octanoyltransferase	Crot	1.058	1.116	1.142	0.914	1.569
1387283_at	myxovirus (influenza virus) resistance 2	Mx2	0.721	0.777	0.503	1.565	1.280
1387307_at	histidine ammonia lyase	Hal	0.903	0.826	0.665	0.819	1.072
1387312_a_at	glucokinase	Gck	1.180	1.610	0.865	0.941	1.077
1387391_at	cyclin-dependent kinase inhibitor 1A	Cdkn1a	1.576	1.373	0.734	0.684	0.892
1387396_at	hepcidin antimicrobial peptide	Hamp	0.731	0.642	1.232	1.145	1.051
1387643_at	fibroblast growth factor 21	Fgf21	1.385	1.919	1.138	1.191	1.157
1387665_at	betaine-homocysteine methyltransferase	Bhmt	1.234	1.064	1.083	0.655	0.850
1387670_at	glycerol-3-phosphate dehydrogenase 2	Gpd2	1.169	1.650	1.430	0.872	0.864
1387730_at	paired box gene 8	Pax8	1.527	1.114	0.991	0.822	0.827
1387809_at	mitogen-activated protein kinase kinase 6	Map2k6	1.017	1.443	1.139	0.622	0.742
1387848_at	3-hydroxy-3-methylglutaryl-Coenzyme A reductase	Hmgcr	0.810	1.306	1.963	1.057	0.876
1388210_at	mitochondrial acyl-CoA thioesterase 1	Mte1	1.085	1.245	1.928	1.099	1.120
1388395_at	G0/G1 switch gene 2 (predicted)	G0s2_predicted	2.129	1.930	1.041	1.204	1.036
1388426_at	sterol regulatory element binding factor 1	Srebf1	0.648	0.787	0.694	0.855	0.885
1388531_at	progesterone receptor membrane component 2 (predicted)	Pgrmc2 predicted	1.032	1.518	1.149	0.938	1.036
1388679_at	TBC1 domain family, member 14 (predicted)	Tbc1d14 predicted	0.815	1.582	1.111	0.883	1.038
1388792_at	growth arrest and DNA-damage-inducible 45 gamma (predicted)	Gadd45 gpredicted	0.340	1.095	0.994	0.669	0.595
1388872_at	Isopentenyl-diphosphate delta isomerase	Idi1	1.029	1.077	1.772	1.249	0.870
1388924_at	angiopoietin-like protein 4	Angptl4	2.172	1.589	1.105	0.673	0.990
1389161_at	Transcribed locus	---	1.547	1.566	1.153	0.819	1.014
1389253_at	vanin 1 (predicted)	Vnn1 predicted	1.127	1.614	1.846	1.232	1.650
1389430_at	Transcribed locus	---	0.917	1.198	1.517	0.863	1.008
1390383_at	adipose differentiation-related protein	ADRP	1.296	1.784	0.870	0.952	0.913
1390607_at	nNOS-intereacting DHHC-containing Dem protein-L	RGD:1303254	0.936	1.463	1.509	0.691	0.878
1390662_at	Ab2-427	---	0.594	0.996	0.819	1.114	0.980
1392607_at	Transcribed locus	---	0.756	0.855	0.725	0.441	1.298

genes were affected by the vehicle (data not shown). Table 1 shows the list of genes that showed at least a 1.5-fold difference between vehicles with $p<0.01$ either in single dose experiment or in the 29th day of repeated dosing. Many of the genes listed are related to lipid metabolism. They were usually up-regulated by corn oil between 3 and 9 h after dosing and returned to the same level or lower at 24 h and at the 29th day. However, there were some exceptional cases, such as aldo-keto reductase 1B7 (down-regulated at 3 and 9 h but up-regulated at 24 h and 29th day), or aldehyde dehydrogenase 1A1 (only up-regulated after repeated administration). Among the genes in Table 1, there are interesting ones, i.e., CYP7A1, CYP8B1, 3-hydroxy-3-methylglutaryl-Coenzyme A reductase, fatty acid synthase, squalene epoxidase, angiopoietin-like protein 4, which are selected and shown as graphs in Fig. 3A–F. The former 5 genes all showed a circadian rhythm in that their expression in the afternoon to the evening was higher than that in the morning to noon. The administration of corn oil appeared to increase this peak. On the other hand, angiopoietin-like protein 4 showed constant expression during the day in methylcellulose, whereas corn oil markedly increased the expression of this gene at 3 and 6 h of administration.

As is obvious from Figs. 1A and 3, there exists a circadian rhythm in rat liver. In order to examine whether the observed changes were due to a disturbance in the basic rhythm, expression of various clock genes were checked and we found that the rhythm (other than that related to lipid metabolism) was relatively unaffected. As typically representative of clock genes, the expression patterns of period 2, D site albumin

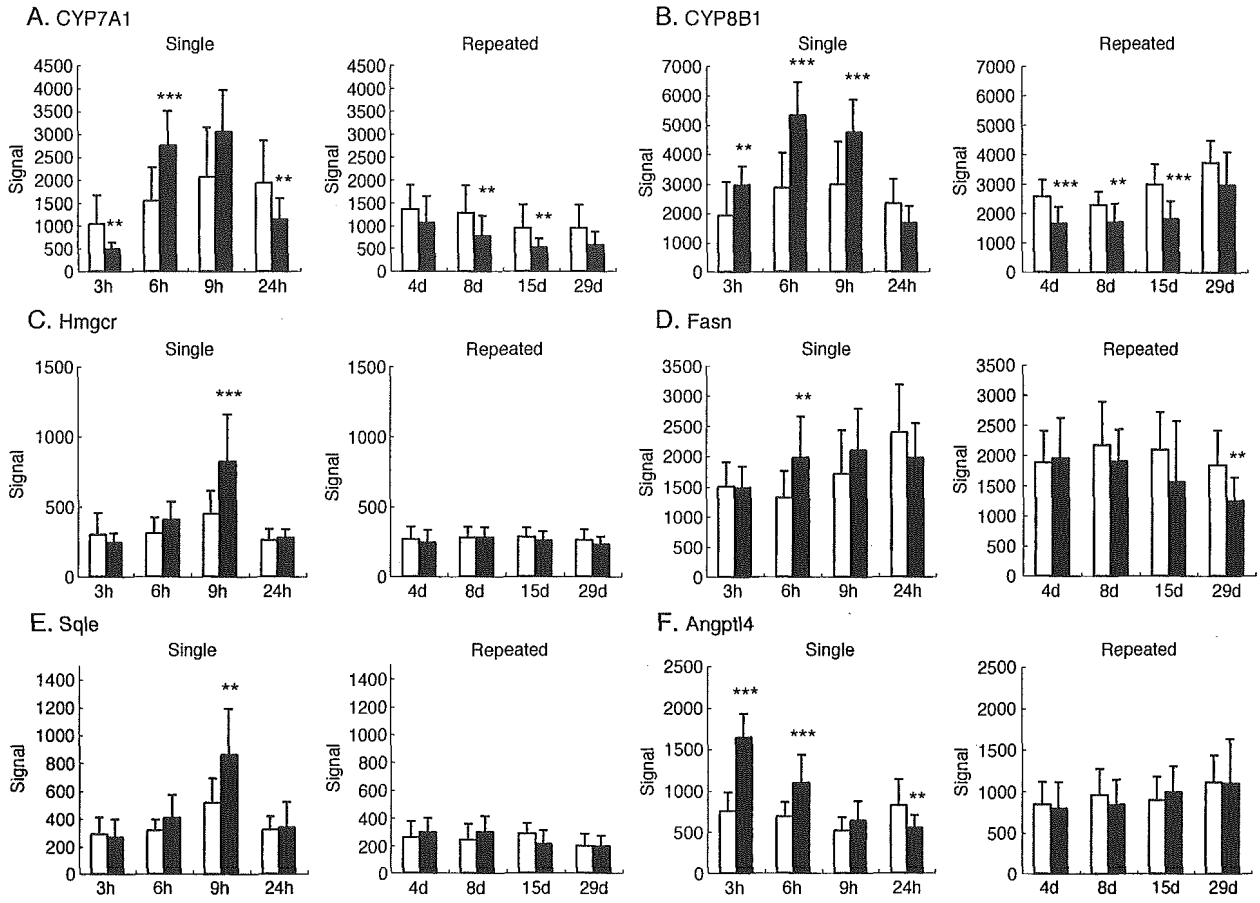

Fig. 3. Expression changes of CYP7A1 (A, Affymetrix ID 1368458_at), CYP8B1(B, Affymetrix ID 368435_at), 3-hydroxy-3-methylglutaryl-Coenzyme A reductase (C, Affymetrix ID 1387848_at), fatty acid synthase (D, Affymetrix ID 1367708_a_at), squalene opixidase (E, Affymetrix ID 1387017_at) and angiopoietin-like protein 4 (F, Affymetrix ID 1388924_at) are shown. Open and filled symbols represent methylcellulose and corn oil, respectively. Values are expressed as mean±SD of 15 rats of each for each time point. Statistically significant between methylcellulose and corn oil by uncorrected Student's *t*-test at $^{**}p<0.01$, $^{***}p<0.001$.

promoter binding protein, and arylhydrocarbon receptor nuclear translocator-like are shown in Fig. 4A–C.

Discussion

The ultimate goal of our project is to create a gene expression database for prediction of hepatotoxicity in the early stage of drug development. For this purpose, it was desirable that the vehicle for suspending drugs was unified to be methylcellulose. However, there are many test compounds with poor dispersibility, and strong detergents or organic solvents are undesirable because of their potent bioactivity, so we inevitably chose corn oil as a vehicle for the highly hydrophobic compounds.

Corn oil contains 9.2 kcal/g and supplies 10.1 kcal/day for 7-week-old rats (5 ml/kg corresponds to 1.1 g for 250 g body weight). Rats around this age consume about 25 g diet per day in the present study (Fig. 1C), which corresponds to about 90 kcal/day (CRF-1 carries 3.6 kcal/g), meaning that the administered corn oil is equal to about 11% of the total calories. Moreover, this is administered once in the morning when the feeding behavior of the rat is normally inactive. Then we were concerned that the difference between corn oil and methylcellulose cannot be ignored. In fact, the food intake of the rats in the corn oil group was significantly decreased by about 15% compared with methylcellulose group without any changes in body weight. This suggests that the rats self-controlled their total calorie intake to a constant level and so corresponding gene expression changes should have occurred.

In the acute phase, total cholesterol, triglyceride, phospholipids, and bilirubin were elevated 3 h after the administration of corn oil, which were considered to be due to rapid absorption of oil. We are not sure why plasma bilirubin was increased; it might reflect an increase in the absorption of bile components when large amounts of lipid were absorbed in the form of micelle. These parameters all returned to the same level as in the methylcellulose group 6–9 h after administration. In the repeated dose experiments, which correspond to 24 h after dosing, triglyceride and bilirubin were decreased in the corn oil group, suggesting that some adapting system lowering plasma lipid was induced during a continuous elevation of lipid component in the diet.

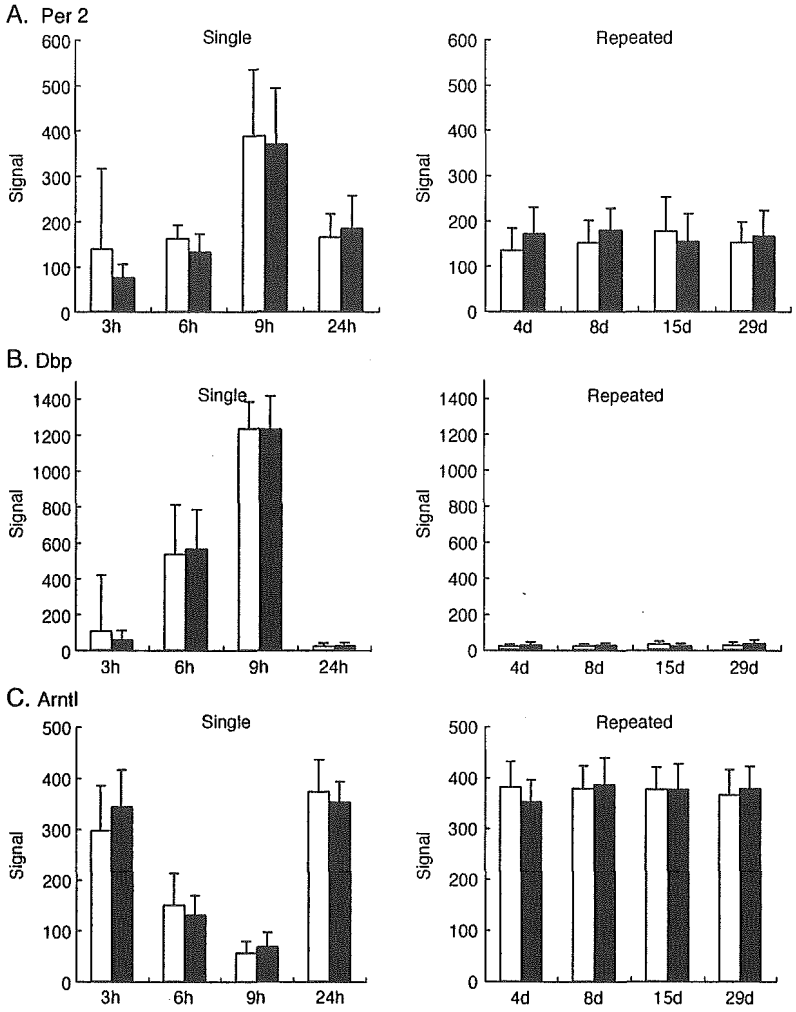

Fig. 4. Expression patterns of representative clock genes, period 2 (A, Affymetrix ID 1368303_at), D site albumin promoter binding protein (B, Affymetrix ID 1387874_at), and arylhydrocarbon receptor nuclear translocator-like (C, Affymetrix ID 1370510_a_at) are shown. Open and filled symbols represent methylcellulose and corn oil, respectively. Values are expressed as mean±SD of 15 rats for each time point. No statistically significant difference was observed between methylcellulose and corn oil at any time point.

The change in gene expression in the liver was more complex. Although the numbers of differentially expressed genes were small in respect of the total 16,000 probe sets, there were still considerable numbers of genes showing different patterns between vehicles, most of which were related to lipid metabolism. In the corn oil-treated group, the expression of CYP7A1 (cholesterol 7α hydroxylase), the rate-limiting enzyme of bile acid synthesis or elimination of cholesterol (Mast et al., 2005), showed a clear circadian rhythm as reported (Kai et al., 1995; Ishida et al., 2000), and it was lower at 3 h but higher at 6 and 9 h than that in the methylcellulose group. The expression was then lowered again at 24 h after dosing, and this pattern appeared to continue during repeated administration, i.e., the expression value in the corn oil group stayed about 60% of those in the methylcellulose group until the 29th day. On the other hand, CYP 8B1 (cholesterol 12α hydroxylase), which catalyzes the synthesis of cholic acid and controls the ratio of cholic acid over chenodeoxycholic acid in the bile, showed a less marked but obvious circadian pattern as reported (Ishida et al., 2000). It showed a continuously higher expression from 3 to 9 h than methylcellulose, returned to the same level at 24 h, and no difference was observed in the repeated dosing. These changes were considered to be the reflection of the transiently high consumption of bile due to the bolus injection of corn oil.

The rate-limiting enzyme of cholesterol biosynthesis, 3-hydroxy-3-methylglutaryl-Coenzyme A reductase, also showed a circadian rhythm and the administration of corn oil markedly increased its expression at 9 h. At this point, squalene epoxidase and sterol-C4-methyloxidase were also increased. The former is a microsomal enzyme that catalyzes the oxidation of squalene to 2,3-oxidosqualene, the last reaction of non-sterol metabolites in the cholesterol biosynthesis pathway (Hidaka et al., 1990). The latter is known as one of the components essential for sterol biosynthesis in yeast (Darnet and Rahier, 2003), and it used to be termed neurorep1 and was discussed in relation to the repair

process of damaged neurons (Uwabe et al., 1997). Looking at the high expression level in liver and induction by corn oil alone, we considered that the induction of sterol-C4-methyloxidase was a general phenomenon related to lipid metabolism rather than neurophysiology.

One noticeable gene is angiopoietin-like protein 4, which was recently shown to be involved not only in lipid metabolism via inhibition of lipoprotein lipase activity (Yoshida et al., 2002) but also in various diseases (Xu et al., 2005). It was reported that its expression in adipose tissue and liver was affected by the nutrient status, e.g., induced by fasting (Ge et al., 2005). In the present study, this gene was markedly up-regulated at 3–6 h after corn oil treatment and returned to the same level as methylcellulose at 9 h or later. It is of interest to elucidate why oil intake resembles fasting in case of angiopoietin-like protein 4 expression.

Fatty acid synthase was up-regulated by corn oil at 6 h after dosing and then returned to the same level as methylcellulose, whereas it was down-regulated (about 60% of methylcellulose) after repeated administration. In contrast, fatty acid binding protein family members, involved in lipid uptake, were up-regulated 24 h after single and repeated administrations of corn oil. These reactions in the repeated phase are considered to be adaptive responses suitable for lipid intake. In addition to these two enzymes, there were genes showing significantly different expression in the corn oil group at 29th day, i.e., serine dehydratase, ornithine aminotransferase, stearoyl CoA desaturase, aldehyde dehydrogenase 1A1, and epoxide hydroxylase 2. Of these, the latter two were up-regulated whereas the others were down-regulated.

The increase of aldehyde dehydrogenase and epoxide hydroxylase is considered to be favorable for the condition of high lipid diet, since both enzymes are reported to be involved in the detoxication of the metabolites associated with lipid metabolism (Choudhary et al., 2005; Newman et al., 2005). As for the down-regulated genes, the decrease of fatty acid synthase and stearoyl CoA desaturase, both are in the pathway of fatty acid synthesis, which might reflect a decrease in the need of fatty acid. Serine dehydratase and ornithine aminotransferase are known to be induced by high protein diet, glucagon, or glucocorticoid (Hunter and Harper, 1977; Bourdel et al., 1983). Based on the present data, it is difficult to conclude whether the change was due to the relative reduction of protein in the diet, or to the secondary change in endocrinological status. Moreover, it should be noted that the circadian pattern could not be obtained in the present experiments of repeated administration. Although most of the observed changes could be interpreted as an adaptation for the rapid absorption of oil from the gut in the acute phase and for the continuously elevated composition of lipid in the food in the chronic phase, it is difficult to map all the changes to various metabolic pathways, and to give reasonable explanations. Further confirmation is obviously needed, but the present study has supplied many valuable suggestions.

Many of the genes affected by corn oil treatment exhibit their own circadian rhythm generally with low expression at 3 h (around noon), increasing from 6 h (late afternoon) to 9 h (evening), and returning to low expression at 24 h (morning) of dosing. There is a long blank period between 9 and 24 h after dosing, as it was practically impossible to perform measurements after midnight in the present project. It was therefore possible that the actual peak of some genes occurred between 9 and 24 h after dosing, or midnight. We were concerned that the compulsory administration of oil in the morning disturbs not only feeding behavior but also the circadian rhythm itself. However, it was confirmed that the expression patterns of representative clock genes were unaffected, suggesting that changes in gene expression were not due to the disturbance of the original circadian rhythm. Moreover, the expression levels of clock genes in repeated dosing (corresponding to the 24 h value) were also unchanged, suggesting that disturbance of the circadian rhythm during repeated administration of oil was unlikely.

The present analysis of the data in our database would provide useful information for future experiments to elucidate the detailed mechanism of lipid metabolism. It also provides valuable information for the analysis of the activity of compounds when a comparison of chemicals dosed with different vehicles is made. Since the data accumulated in our database appeared to be of high quality and reproducibility, at least in terms of the effect of vehicles, we expect that drug actions, especially related to toxicity, may be sensitively detected using our database.

Acknowledgements

This study was supported in part by a grant from the Ministry of Health, Labour and Welfare (H14-Toxico-001).

References

Bourdel, G., Hitier, Y., Lardeux, B., Girard-Globa, A., 1983. Activity of several enzymes of amino acid catabolism in the liver of rats fed protein as a meal. Reproduction Nutrition Development 23, 875–881.

Choudhary, S., Xiao, T., Srivastava, S., Zhang, W., Chan, L.L., Vergara, L.A., Van Kuijk, F.J., Ansari, N.H., 2005. Toxicity and detoxification of lipid-derived aldehydes in cultured retinal pigmented epithelial cells. Toxicology and Applied Pharmacology 204, 122–134.

Darnet, S., Rahier, A., 2003. Enzymological properties of sterol-C4-methyl-oxidase of yeast sterol biosynthesis. Biochimica et Biophysica Acta 1633, 106–117.

Ge, H., Cha, J.Y., Gopal, H., Harp, C., Yu, X., Repa, J.J., Li, C., 2005. Differential regulation and properties of angiopoietin-like proteins 3 and 4. Journal of Lipid Research 46, 1484–1490.

Hidaka, Y., Satoh, T., Kamei, T., 1990. Regulation of squalene epoxidase in HepG2 cells. Journal of Lipid Research 31, 2087–2094.

Hunter, J.E., Harper, A.E., 1977. Induction of pyridoxal phosphate-dependent enzymes in vitamin B-6 deficient rats. Nutrition 107, 235–244.

Ishida, H., Yamashita, C., Kuruta, Y., Yoshida, Y., Noshiro, M., 2000. Insulin is a dominant suppressor of sterol 12 alpha-hydroxylase P450 (CYP8B) expression in rat liver: possible role of insulin in circadian rhythm of CYP8B. Journal of Biochemistry (Tokyo) 127, 57–64.

Kai, M.-H., Eto, T., Kondo, K., Setoguchi, Y., Higashi, S., Maeda, Y., Setoguchi, T., 1995. Synchronous circadian rhythms of mRNA levels and activities of cholesterol 7 alpha-hydroxylase in the rabbit and rat. Journal of Lipid Research 36, 367–374.

Mast, N., Graham, S.E., Andersson, U., Bjorkhem, I., Hill, C., Peterson, J., Pikuleva, I.A., 2005. Cholesterol binding to cytochrome P450 7A1, a key enzyme in bile acid biosynthesis. Biochemistry 44, 3259–3271.

Newman, J.W., Morisseau, C., Hammock, B.D., 2005. Epoxide hydrolases: their roles and interactions with lipid metabolism. Progress in Lipid Research 44, 1–51.

Urushidani, T., Nagao, T., 2005. Toxicogenomics: the Japanese initiative. In: Borlak, J. (Ed.), Handbook of Toxicogenomics—Strategies and Applications. Wiley-VCH, pp. 623–631.

Uwabe, K., Gahara, Y., Yamada, H., Miyake, T., Kitamura, T., 1997. Identification and characterization of a novel gene (neurorep 1) expressed in nerve cells and up-regulated after axotomy. Neuroscience 80, 501–509.

Waring, J.F., Ulrich, R.G., Flint, N., Morfitt, D., Kalkuhl, A., Staedtler, F., Lawton, M., Beekman, J.M., Suter, L., 2004. Interlaboratory evaluation of rat hepatic gene expression changes induced by methapyrilene. Environmental Health Perspectives 112, 439–448.

Xu, A., Lam, M.C., Chan, K.W., Wang, Y., Zhang, J., Hoo, R.L., Xu, J.Y., Chen, B., Chow, W.S., Tso, A.W., Lam, K.S., 2005. Angiopoietin-like protein 4 decreases blood glucose and improves glucose tolerance but induces hyperlipidemia and hepatic steatosis in mice. Proceedings of the National Academy of Sciences of the United States of America 102, 6086–6091.

Yoshida, K., Shimizugawa, T., Ono, M., Furukawa, H., 2002. Angiopoietin-like protein 4 is a potent hyperlipidemia-inducing factor in mice and inhibitor of lipoprotein lipase. Journal of Lipid Research 43, 1770–1772.

Available online at www.sciencedirect.com
SCIENCE DIRECT®
Leukemia Research 29 (2005) 933–942
Leukemia Research
www.elsevier.com/locate/leukres

Resistance against Friend leukemia virus-induced leukemogenesis in DNA-dependent protein kinase (DNA-PK)-deficient *scid* mice associated with defective viral integration at the *Spi-1* and *Fli-1* site

Maki Hasegawa [a], Shuichi Yamaguchi [a], Shiro Aizawa [b], Hidetoshi Ikeda [c], Kouichi Tatsumi [b], Yuko Noda [b], Katsuiku Hirokawa [a], Masanobu Kitagawa [a,*]

[a] *Department of Comprehensive Pathology, Aging and Developmental Sciences, Tokyo Medical and Dental University, Graduate School, 1-5-45 Yushima, Bunkyo-ku, Tokyo 13-8519, Japan*
[b] *Research Center for Radiation Safety, National Institute of Radiological Sciences, 4-9-1 Anagawa, Inage-ku, Chiba 263-8555, Japan*
[c] *Laboratory of Infectious Diseases, National Institute of Animal Health, 3-1-5 Kannondai, Tsukuba City, Ibaraki 305-0856, Japan*

Received 5 October 2004; accepted 22 January 2005
Available online 11 March 2005

Abstract

Retroviral DNA integration is mediated by the viral protein integrase. However, elements of the host DNA repair machinery such as the phosphatidylinositol 3-kinase (PI-3K)-related protein kinase family system would play a role in the integration of viral DNA into the host DNA. Here, we show that a host PI-3K-related protein kinase, DNA-dependent protein kinase (DNA-PK), plays a role in the specific integration of retroviral DNA and induction of retroviral diseases in vivo. DNA-PK-deficient *scid* mice inoculated with Friend leukemia virus (FLV) exhibited a random integration into their genomic DNA and expressed the viral envelope protein gp70. However, the specific integration of FLV at *Spi-1* or *Fli-1* sites did not occur in association with the significant resistance of *scid* mice to FLV-induced leukemogenesis. In contrast, the knockout of another member of the PI-3K-related protein kinase family, encoded by the *ataxia telangiectasia mutated* (*ATM*) gene, resulted in mice as sensitive to FLV-induced leukemogenesis as the wild type mice. FLV was specifically integrated into the DNA at *Spi-1* and *Fli-1* sites with significant expression of these transcription factors. These findings indicated that DNA-PK would be essential for controlling the in vivo integration of FLV at specific sites as well as the susceptibility to FLV-induced leukemogenesis.

Keywords: Retrovirus infection; Friend virus; DNA-PK; ATM; Integration

1. Introduction

Integration into the host DNA is an essential step in retroviral replication [1]. The integration of retroviral DNA is usually mediated by the viral protein integrase [2,3]. However, recent in vitro studies suggest that several host proteins also participate in the reaction. Daniel et al. [4] have reported that the integrase-mediated joining of retroviral and host DNA is recognized as damage by the host cells, and that DNA repair proteins, such as DNA-dependent protein kinase (DNA-PK), may be required to facilitate stable integration. The catalytic subunit of DNA-PK, DNA-PKcs, is a member of a family of large, presumably multifunctional, phosphatidylinositol 3-kinase (PI-3K)-related protein kinases [5,6]. DNA-PKcs is a component of the cellular, non-homologous end-joining (NHEJ) pathway and is known to be required for the repair of double-strand breaks induced by ionizing radiation and certain DNA-damaging drugs and for V(D)J recombination during the generation of immunoglobulin-producing cells [7]. The initial events in retroviral integration would be detected as DNA damage by the host cell and DNA-PK-mediated repair may be required for the completion of the integration process. Thus, DNA-PK-deficient murine *scid* cells infected with retroviruses showed a substantial reduction in retroviral DNA integration as compared with control cells because

* Corresponding author. Tel.: +81 3 5803 5399; fax: +81 3 5803 0123.
E-mail address: masa.pth2@med.tmd.ac.jp (M. Kitagawa).

0145-2126/$ – see front matter © 2005 Elsevier Ltd. All rights reserved.
doi:10.1016/j.leukres.2005.01.016

the abortive integration of retroviruses induced apoptosis [8]. However, other experiments using HIV-1-derived retroviral vectors and cultured *scid* cells revealed that DNA-PK is not required for efficient retroviral integration [9]. Thus, the roles of DNA-PK in the retroviral integration are still unclear.

The *ataxia telangiectasia mutated* (*ATM*) gene and the *ATM* and *Rad3*-related (*ATR*) gene, which also encode members of the PI-3K-related protein kinase family, play important roles in inducing cell cycle arrest in response to DNA damage and partially contribute to DNA repair. Using wortmannin (an irreversible inhibitor of PI-3K-related protein kinases including DNA-PK and ATM kinases) and a DNA-PK-deficient murine *scid* cell system, Daniel et al. [8] have shown that in the absence of DNA repair protein of the NHEJ pathway, ATM is required to allow stable retroviral integration and to avoid integrase-mediated cell killing. However, recent in vitro experiments using caffeine (an efficient inhibitor of ATM and ATR) and an ATM-deficient cell system demonstrated that ATR kinase activity was required for successful completion of the integration [10]. Thus, the identity and mechanism of action of proteins responsible for repair of the viral–host DNA in the retroviral integration process have differed among the experimental systems employed.

To clarify the overall contribution of PI-3K-related protein kinases to the retroviral integration process and their significance for retrovirus-induced pathogenesis, it is important to trace the overall process of retroviral infection in the in vivo system using PI-3K-related protein kinase-deficient hosts. Thus, in the present study, Friend leukemia virus (FLV) was introduced into DNA-PK-deficient *scid* mice and *ATM* knockout (−/−) mice with the C3H background although regrettably, the knockout of *ATR* is embryonic lethal [11]. The FLV-induced leukemogenicity in these in vivo systems was determined and retroviral infection-related events in these PI-3K-related protein kinase-deficient mice were analyzed.

2. Materials and methods

2.1. Mice

The 8–10-week-old male C3H/He (C3H) mice were bred from our colony at the Animal Production Facility of the National Institute of Radiological Sciences in Chiba. The *scid* mice and *ATM* knockout (−/−) mice with the C3H background were also bred from our colony. Methods for the generation of knockout constructs and *ATM* −/− mice were described elsewhere [12]. The *scid* and *ATM* −/− mice with the C3H background were generated by crossing CB.17 *scid* and 129/Sv *ATM* −/− mice [13] with the C3H strain, respectively, followed by backcrossing through more than 20 generations. All mice were maintained within a barrier-sustained specific-pathogen-free (SPF) facility. All animals were reared and treated in accordance with the guidelines governing the care and use of laboratory animals at the National Institute of Radiological Sciences (approval numbers 1997-4 and 1997-17) and also the guidelines established by the Animal Experiment Committee of the Tokyo Medical and Dental University.

2.2. Viral infection and determination of leukemogenesis

An NB-tropic Friend leukemia virus complex, originally provided by Dr. C. Friend, was prepared as described earlier [14] and injected i.p. into mice at a highly leukemogenic dose of 10^4 PFU/mouse [15]. The development of leukemia was assessed using the hematocrit (Ht) value (%) and the nucleated cell count (NCC) of peripheral blood from the tail vein ($\times 10^3/mm^3$) after inoculation with FLV. One, 2, 4 and 8 weeks after the inoculation, spleen cells were collected from experimental groups of mice, stained with phycoerythrin (PE)-conjugated monoclonal anti-erythroid cells (TER119, Pharmingen, San Diego, CA, USA), and analyzed on a FACScan (Becton Dickinson Immunocytometry Systems, Mountain View, CA, USA). The TER119-positive cell parameter was calculated [16].

2.3. Southern blot hybridization

To detect the integration of proviral DNA into spleen cells from the FLV-infected mice, Southern blot hybridization was performed for FLV-specific sequences of cellular DNA [17]. Chromosomal DNA was extracted from the spleen by the phenol extraction method [18] with modifications. The DNA (10 μg) digested with restriction enzymes was fractioned by electrophoresis through 0.7% agarose gel, transferred to a Magna nylon membrane (Micron Separations Inc., Westboro, MA, USA), and hybridized to a ^{32}P-labeled *env* probe derived from a 0.8-kb *Bam*HI–*Bam*HI fragment of the Friend MuLV *env* region [19]. Southern hybridization and washing were performed according to the manufacturer's instructions (Micron Separations Inc.). Briefly, hybridization was carried out at 65 °C for 16 h in 5× SSPE, 5× Denhardt's solution, 0.5% SDS and 10 μg/ml of heat denatured salmon sperm DNA. Washing was carried out at room temperature for 10 min in 2× SSC, at 65 °C for 60 min in 2× SSC and 0.5% SDS, and then at room temperature for 10 min in 0.1× SSC. Hybridization and washing were done in rotation in a hybridization oven. Hybridization signals were detected by exposing the imaging plate of a Bio Imaging Analyzer (Fuji Bas 2000, Tokyo, Japan). Because *Hin*dIII cut the Friend MuLV sequences at two sites outside of the probe-binding portion, randomly integrated viral DNA would be detected as smears. In contrast, *Bam*HI digestion cut both ends of the probe-binding portion because the probe was designed from a *Bam*HI–*Bam*HI fragment of Friend MuLV. Therefore, *Bam*HI digestion would demonstrate integrated viral DNA.

2.4. Direct PCR for detecting specific integration of FLV at the Spi-1 or Fli-1 site

To determine the precise location and transcriptional orientation of the proviruses, we directly amplified junc-

tion fragments of proviral and host DNA using proviral primers and flanking host DNA primers. These primers were synthesized by a commercial laboratory (Invitrogen Corp., Carlsbad, CA, USA). The following pairs of primers were used: a primer from the LTR of F-MuLV, P3, *F-MuLV-P3*: GTCGCCCGGGTACCCGTATTC, and a primer from the sequence of the F-MuLV integration site of *Fli-1*, *Fli-1-Pu*: CGCTGAAGGGAAGAGCAAGAG [26], and in the same way, that of *SFFF-P3*: CACTAGAATACGAGCCACGATAAAT, and that of the SFFV integration site, *Spi-1*, *Spi-1-Pu*: CTTTCACTTGTGTAGTTGAAGATGG. High molecular weight DNAs (150 ng) were subjected to 35 cycles of PCR in a final volume of 50 μl, containing 0.2 mM of each dNTP, 1 mM $MgSO_4$, 1.0 unit of KOD-Plus-DNA polymerase (Toyobo, Osaka, Japan) and 1× PCR buffer for KOD-Plus-DNA polymerase, and 0.3 μM of each primer. PCR was performed for 35 cycles of 1 min at 94 °C, 30 s at 60 °C and 3 min at 68 °C. Aliquots of 10 μl were analyzed by electrophoresis in 1.0 or 1.5% agarose gels and visualized using ethidium bromide fluorescence. λ/*Hin*dIII–*Eco*RI-cut DNA or *ϕXHae*III-cut DNA was run in parallel as a molecular weight marker.

2.5. Reverse transcription (RT)-polymerase chain reaction (PCR) for Spi-1 or Fli-1 expression

To determine the activation of the *Spi-1* and *Fli-1* genes which is essential for the transformation of erythroid cells during the progression of FLV-induced disease [20], RT-PCR was performed in each experimental group. The RNA was extracted from the spleen and bone marrow using an RNeasy Mini Kit (Qiagen, Valencia, CA, USA) according to the manufacturer's directions. Tissue RNA (100 ng) was used as a template for the amplification reactions. Complementary (c) DNA was synthesized using Rous-associated virus reverse transcriptase (Takara Biomedicals, Kyoto, Japan). The PCR was performed as described elsewhere [21]. Oligonucleotides as specific primers for *Spi-1* and *Fli-1* were synthesized by a commercial laboratory (Life Technologies Oriental, Tokyo, Japan). As a control reaction, β-actin was also included in each run. The sequences of primers were as follows: *Spi-1*: 5′ PCR primer ATGGAAGGGTTTTCCCTCACCGCC, 3′ PCR primer CTGCACGCTCTGCAGCTCTGTGAA; *Fli-1*: 5′ PCR primer CCAGAACATGGATGGCAAGGA, 3′ PCR primer CCCAGGATCTGATAAGGATCTGGC; β-actin: 5′ PCR primer TGGAATCCTGTGGCATCCATGA, 3′ PCR primer ATCTTCATGGTGCTAGGAGCCAG. The expected sizes of the PCR products were 216 bp for *Spi-1*, 324 bp for *Fli-1* and 175 bp for β-actin. *ϕX174/Hae*III-cut DNA was run in parallel as a molecular weight marker.

2.6. Bone marrow transplantation (BMT)

To determine whether hematopoietic cells of the *scid* mice were actually refractory to FLV-induced leukemia even under conditions of normal NK-cell activity, a BMT model to rescue the FLV-infected wild type C3H host was generated. The wild type C3H mice that had a normal immune function, in other words, that did not have elevated NK-cell activity, were inoculated with FLV. One week later when FLV-induced splenomegaly was evident, mice were lethally irradiated (9.5 Gy) and transplanted with 10^6 of bone marrow cells from C3H *scid* mice. As control experiments, FLV-free C3H mice transplanted with the C3H *scid* bone marrow cells and FLV-inoculated C3H mice transplanted with the wild type C3H bone marrow cells were also generated.

2.7. Detection of apoptosis

Fresh spleen tissue was mounted in an OCT compound (Sakura, Tokyo, Japan), frozen with liquid nitrogen and cut to make 8–10 μm thick frozen sections. To identify apoptotic cells on frozen tissue sections by terminal deoxytransferase (TdT)-mediated dUTP nick end labeling (TUNEL), an in situ cell death detection kit, fluorescein (Boeringer Mannheim, Mannheim, Germany) was used as described previously [22]. Briefly, frozen sections were fixed with a 4% paraformaldehyde solution for 20 min, washed with phosphate-buffered saline (PBS), incubated in 0.1% sodium citrate–0.1% Triton X-100 for 2 min, washed with PBS and then incubated with FITC-labeled dUTP and TdT at 37 °C for 60 min. Sections were then observed under a fluorescent microscope and the TUNEL-positive cell ratio was determined by dividing the number of positively stained cells by the total cell number (counting more than 1000 cells).

2.8. Western blot analysis for gp70 and p53 protein

Spleen cells from each group of mice were suspended in Iscove's modified Dulbecco's medium (IMDM, Sigma, St. Louis, CA, USA) containing 10% fetal bovine serum, at a concentration of 6×10^6 cells/tube and pelleted. Cell lysates were prepared by incubating the pellets on ice for 15 min in 1 ml of a lysis buffer containing 10 mM Tris–HCl (pH 7.5), 5 mM EDTA, 1% Nonidet P-40, 0.02% NaN_3, 1 mM phenylmethyl sulfonyl fluoride (PMSF), 0.1% aprotinin 100 μM leupeptin, and 100 μM tosyl-L-phenylalanyl chloromethyl ketone (TPCK) (Sigma). Supernatants were separated from debris by centrifugation at 12,000 rpm (9000 × *g*) for 5 min at 4 °C. Protein concentrations were determined using a Bio-Rad protein assay kit (Bio-Rad Laboratories, Hercules, CA, USA). The whole cell lysate (50 μg) was subjected to 8, 10 or 12.5% SDS-PAGE. Gels were transferred electrophoretically to nitrocellulose membranes (Schleicher and Schull, Dassel, Germany). The membranes were blocked in 10% skim milk in PBS, incubated with a goat polyclonal anti-gp70 (Quality Biotech, Camden, NJ, USA) or a mouse monoclonal antibody to P53 protein (Pab 240, Santa Cruz Biotechnology, Santa Cruz, CA, USA), and after being washed were incubated with a horseradish peroxidase-conjugated anti-

Table 1
Hematocrit (Ht) value of the peripheral blood from the wild type, *scid* and *ATM* −/− mice after inoculation with FLV

Mice	Time after inoculation with FLV				
	Control	1 Week	2 Weeks	4 Weeks	8 Weeks
C3H wild	51 ± 1.0	48 ± 1.0	38 ± 2.0	31 ± 4.3	21 ± 5.5[a]
C3H *scid*	46 ± 0.7	43 ± 1.5	41 ± 0.3	36 ± 3.8	38 ± 1.6[a,b]
C3H *ATM* −/−	45 ± 2.6	48 ± 5.0	42 ± 1.5	30 ± 1.7	23 ± 6.4[b]

Values indicate the mean ± S.D. of the Ht value (%) of peripheral blood in three to five mice from each experimental group. Note the gradual decrease in the Ht value of wild type and *ATM* −/− mice, 2 and 4 weeks after FLV inoculation, in contrast to the slight increase or normal level in the FLV-inoculated *scid* mice.
[a] Differences were significant between the C3H control and *scid* mice at 8 weeks after FLV inoculation using Student's *t*-test ($p < 0.01$).
[b] Differences were significant between the *scid* and *ATM* −/− mice at 8 weeks after FLV inoculation using Student's *t*-test ($p < 0.01$).

goat or anti-mouse IgG antibody (Dakopatts, Glostrup, Denmark). To confirm the equivalent loading of protein in each lane, membranes were blocked, incubated in polyclonal rabbit anti-actin antisera (Sigma), and after washing, incubated in horseradish peroxidase-conjugated anti-rabbit Ig antibody (Dakopatts). Bands in the washed membrane were detected with an enhanced chemiluminescence (ECL) system (Amersham Life Science, Buckinghamshire, UK) as described previously [22].

2.9. Densitometric analysis

The densities of bands were measured by densitometric analysis with an ImageQuant scanning imager (Molecular Dynamics, Sunnyvale, CA, USA). The relative intensities of the bends were calculated by comparing the density of the sample with that of the control.

3. Results

3.1. FLV-induced leukemogenesis in the scid and ATM −/− mice

First, to determine the leukemogenicity of FLV in DNA-PK-deficient *scid* mice and *ATM* −/− mice, parameters including the hematocrit (Ht) value, nucleated cell count (NCC) of peripheral blood, spleen weight and TER119-positive cell ratio of the spleen were determined after inoculation with a leukemogenic dose of FLV. As shown in Table 1, Ht values declined remarkably after FLV inoculation in the wild type and *ATM* −/− C3H mice. In contrast, the *scid* mice showed only a slight decrease in the Ht value. Regarding the NCC, spleen weight and TER119-positive cell ratio, FLV-inoculated wild type and *ATM* −/− mice showed a gradual but significant increase after the inoculation with FLV, while *scid* mice showed very slow or no remarkable change (Fig. 1). As shown in Fig. 2, all the FLV-inoculated wild type mice died from leukemia within 19 weeks and the *ATM* −/− mice within 15 weeks, while only 20% of the FLV-inoculated *scid* mice died from leukemia; the majority of mice lived for more than 24 weeks with no evidence of splenomegaly. The *ATM* −/− mice seemed more susceptible to FLV-induced leukemia than the wild type mice probably due to their immunodeficient nature [23,24]. These findings indicated that FLV inoculation induced leukemia in the wild type and *ATM* −/− mice, whereas, the *scid* mice were significantly refractory to FLV-induced leukemogenesis.

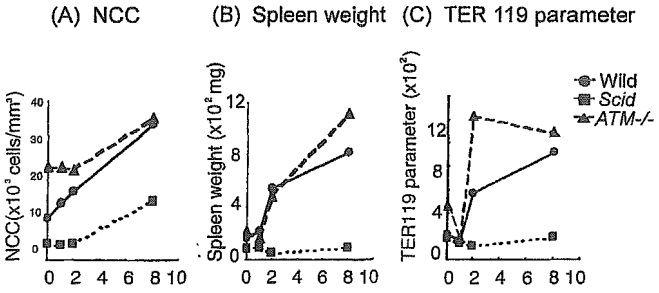

Fig. 1. FLV-induced leukemogenicity in mice with the C3H background. Lines indicate the wild type (●), *scid* (■) and *ATM* −/− mice with the C3H background (▲). Parameters for the leukemogenicity are: (A) nucleated cell count of peripheral blood ($\times 10^3$/mm^3); (B) spleen weight ($\times 10^2$ mg); (C) TER119-positive cell parameter of the spleen (spleen weight (mg) × TER119-positive cell ratio (%)/body weight (g)). Note that FLV-inoculated wild type mice and *ATM* −/− mice exhibited an increase in these parameters indicating the induction of leukemia, 4 and 8 weeks after inoculation with FLV, while *scid* mice revealed only a slight increase in each parameter.

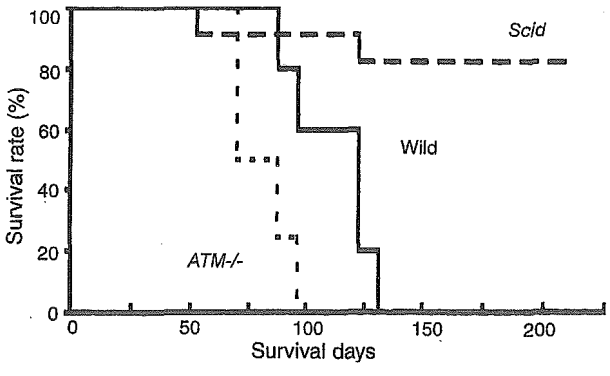

Fig. 2. Survival curves of the mice with the C3H background after inoculation with FLV. Lines indicate the wild type (solid line, $n = 10$), *scid* (broken line, $n = 13$) and *ATM* −/− (dotted line, $n = 8$) mice with the C3H background. Note the significantly longer survival of the FLV-inoculated *scid* mice compared with the FLV-inoculated wild type or *ATM* −/− mice ($p < 0.01$ and $p < 0.001$ using the Mantel–Cox test, respectively). In addition, the survival of *ATM* −/− mice was significantly shorter than that of wild type mice ($p < 0.05$).

3.2. Integration of FLV in spleen cells from the FLV-infected scid and ATM −/− mice

To investigate the actual integration of FLV into the host DNA of the *scid* and *ATM* −/− mice, Southern blot hybridization was performed to detect FLV-specific sequences in the host genome. As shown in Fig. 3A, randomly integrated FLV sequences were detected by *Hin*dIII digestion as smears, and as shown in Fig. 3B, *Bam*HI digestion demonstrated the overall integrated sequences as clear bands in spleens from the wild type and *ATM* −/− mice, 1 and 4 weeks after inoculation with FLV. Integrated signals were also clearly detected in samples from the *scid* mice, although the densities of the bands were slightly weaker. Analysis using densitometry revealed that the intensity of integration signals in *scid* mice was 2–3-fold less than those of wild mice and that the intensities in *ATM* −/− mice was almost two thirds of those of wild mice. These results suggested that the random integration of FLV did occur in the wild type and *ATM* −/− mice and also in the *scid* mice as well, although the integration efficiency seemed lower especially in *scid* mice.

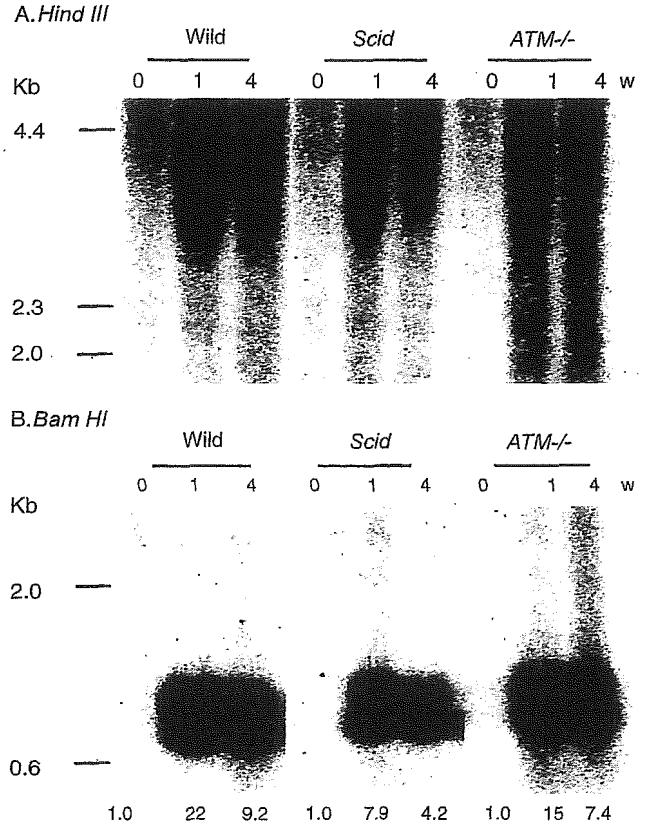

Fig. 3. Southern blot hybridization analysis for FLV-specific sequences in host DNA of the wild type, *scid* and *ATM* −/− mice after inoculation with FLV. Genomic DNA (10 μg) of high molecular weight prepared from each experimental group of mice was digested with *Hin*dIII (A) and *Bam*HI (B). Each sample was hybridized with a ^{32}P-labeled Friend MuLV-derived DNA probe. *Hin*dIII digestion was expected to detect randomly integrated F-MuLV DNA as smears and free viral cDNA as bands. In contrast, *Bam*HI digestion would reveal integrated or free DNA as distinct bands. As we could detect smear signals but not band signals in *Hin*dIII digestion experiments, free viral cDNA would be ignorable probably because we prepared the samples by a high molecular weight DNA extraction method. Note that the integrated proviral sequences of F-MuLV were prominent in the wild type and *ATM* −/− mice, 1 and 4 weeks after inoculation with FLV. The *scid* mice also demonstrated significant integration although the density of bands appeared slightly weaker. The relative intensities of bands were measured by densitometry (wild mouse sample before inoculation with FLV as the control, 1.0) and indicated under the photos of gels.

3.3. Expression of gp70 protein in spleen cells of the wild type, scid and ATM −/− mice

To confirm whether the integrated viral genes were actually expressed, the viral envelope protein gp70, was examined by Western blotting after inoculation of the wild type and *scid* mice. As shown in Fig. 4, gp70 was abundantly expressed in the spleen cells of wild type mice, 1, 4 and 8 weeks after the inoculation with FLV. In the *scid* mice also, spleen cells exhibited significant signals at 1, 4 and 8 weeks, although the expression of gp70-associated protein was observed as early as 1 and 3 days in *scid* mice. However, the overall expression of gp70 was slightly lower in the *scid* mice than the wild type mice. These findings were consistent with the data shown in Fig. 3A and B indicating the levels of FLV integration into spleen cells of the wild type and *scid* mice.

3.4. Integration of FLV at Spi-1 and Fli-1 sites and the expression of Spi-1 and Fli-1 in spleen cells of the wild type, scid and ATM −/− mice

Spi-1 and *Fli-1* are transcription factors expressed in the majority of FLV-induced leukemia cells [25,26]. Integration of the spleen focus forming virus (SFFV) occurs at the *Spi-1* site and that of the Friend murine leukemia virus (MuLV) adjacent to the *Fli-1* site. The integrated LTR of the virus promotes the expression of these transcription factors causing leukemogenesis. To detect the specific integration of viral sequences at these sites, direct PCR analysis was performed using primer sets amplifying junction fragments of the integrated viral sequences and the host transcription factor sequences. As shown in Fig. 5A, dilution experiments were performed using PCR products for the *Spi-1* site detected 1 week after inoculation with FLV and those for the *Fli-1* site by week 8 in spleen cells of the wild type mice. Both signals were evident in 5× and 1× (no dilution) samples. Then, the PCR was performed for samples from 0, 1 and 8 weeks after inoculation with FLV in wild type, *scid* and *ATM* −/− mice. As shown in Fig. 5B, PCR products for the *Spi-1* site were detected 1 week after inoculation with FLV and those for the *Fli-1* site by week 8 in spleen cells of the wild type and *ATM* −/− mice, These findings indicate that the monoclonal expansion of leukemic cells occurs with integration of SFFV at the *Spi-1* site at an early stage and later with the integration of F-MuLV at the *Fli-1* site. In contrast, spleen cells from the *scid* mice exhibited a very weak signal for *Spi-1* site integration and the undetectable level of *Fli-1* site integration signal

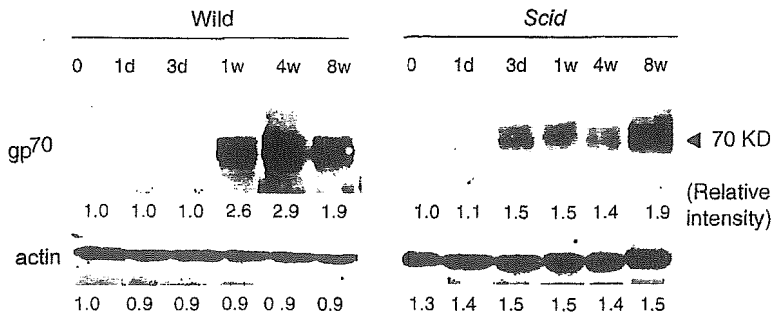

Fig. 4. Expression of gp70 in the C3H wild type and *scid* mice determined by Western blotting. The relative intensities of bands were measured by densitometry (0 day, wild type as the control, 1.0) and indicated under the photos of gels. Note that the expression of gp70 was prominent in the wild type mice, 1, 4 and 8 weeks after inoculation with FLV. The *scid* mice expressed gp70 from the earlier period after FLV inoculation (1 and 3 days) probably originated from the immunodeficient nature of these mice. In 1, 4 and 8 weeks, *scid* mice demonstrated significant expression although the density of bands in 1 and 4 weeks appeared slightly weaker than the wild type.

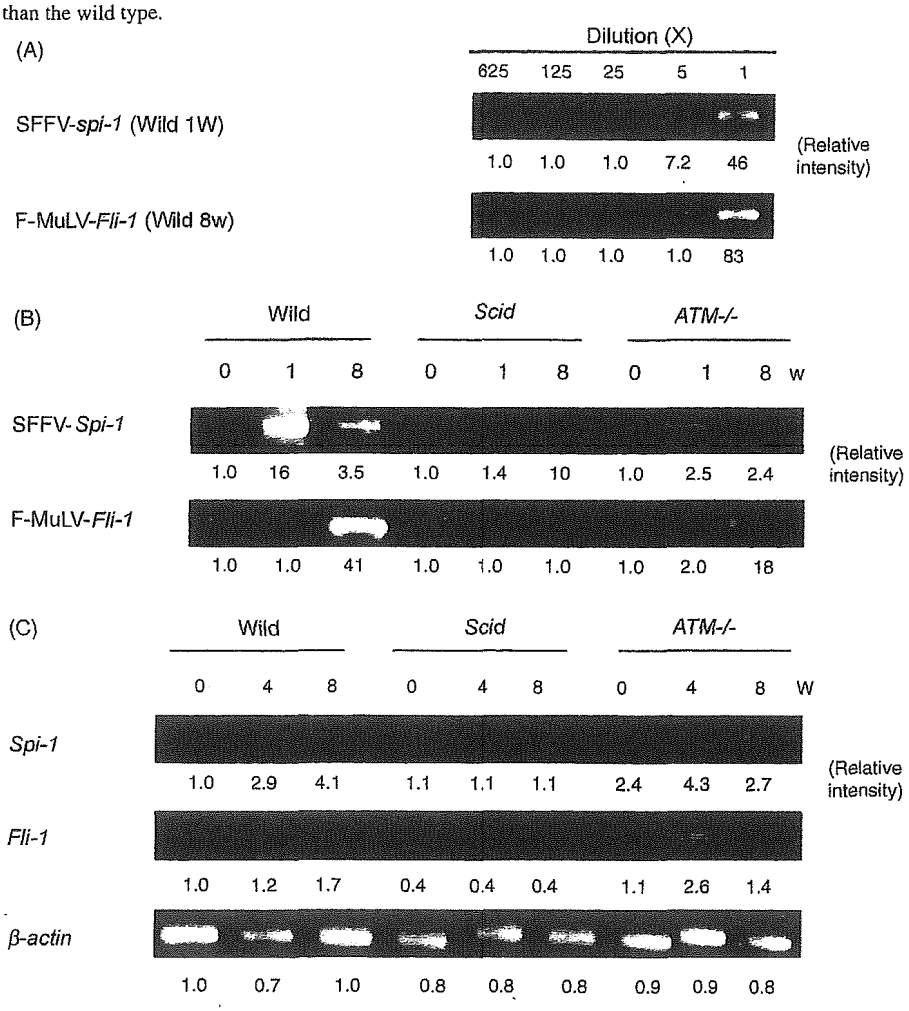

Fig. 5. Specific integration of FLV and expression of the transcription factors. Direct PCR analysis for the specific integration of FLV at the *Spi-1* or *Fli-1* site (A) and RT-PCR analysis for the mRNA expression of *Spi-1* and *Fli-1* (B) in the spleen of mice with the C3H background. DNA or RNA samples were prepared from the spleen of wild type, *scid* and *ATM* −/− mice, before and 1 and 8 weeks after inoculation with FLV. (A) DNA samples from wild type mice were prepared 1 and 8 weeks after inoculation with FLV and diluted to 5×, 25×, 125× and 625×. Direct PCR was performed for SFFV-*Spi-1* in samples from week 1 with each dilution or F-MuLV-*Fli-1* in samples from week 8. The relative intensities of bands were measured by densitometry (625× sample as the control, 1.0) and indicated under the photos of gels. Note that both signals were evident in samples 5× and 1×. (B) Direct PCR exhibited integration of SFFV at the *Spi-1* site (1 week after FLV inoculation) and F-MuLV at the *Fli-1* site (4 weeks after FLV inoculation) in spleen cells from the wild type and *ATM* −/− mice. In contrast, very weak signal was observed in spleen cells from the *scid* mice for *Spi-1* site integration and the signal was not detectable for the *Fli-1* site integration. The relative intensities of bands were measured by densitometry (0 day, wild type as the control, 1.0) and indicated under the photos of gels. (C) A RT-PCR technique revealed overexpression of mRNA for *Spi-1* and *Fli-1* in the FLV-infected wild type and *ATM* −/− samples, 4 and 8 weeks after FLV inoculation. However, up-regulation was not detectable in samples from FLV-inoculated *scid* mice. The relative intensities of bands were measured by densitometry (0 day, wild type as the control, 1.0) and indicated under the photos of gels.

suggesting that the cells with viral integration at *Spi-1* as well as *Fli-1* site did not show progressive proliferation after FLV inoculation. The defective integration of FLV to these specific sites may be related to the lower level of overall random integration in *scid* mice.

To determine whether the FLV-induced disease-specific transcription factors were activated by infection with FLV, mRNA levels of *Spi-1* and *Fli-1* was examined in spleen cells from the wild type, *scid* and *ATM* −/− mice using the RT-PCR technique. The expression of mRNA for *Spi-1* and *Fli-1* (Fig. 5C) was significantly up-regulated in FLV-inoculated wild type and *ATM* −/− mice, 4 and 8 weeks after the inoculation with FLV, as compared with the control (non-inoculated) mice. In contrast, the *scid* mice did not exhibit the expression of *Spi-1* and *Fli-1* after the inoculation. These results confirmed that FLV-infection actually evoked leukemogenesis indicated by the expression of FLV-induced disease-specific transcription factors in spleen cells of the wild type and *ATM* −/− mice but not of the *scid* mice.

3.5. Effects of scid bone marrow transplantation in the FLV-infected C3H mice

To explain the FLV-resistance of *scid* mice by the defective integration of SFFV and F-MuLV to the specific sites, several possibilities should be ruled out. One of these would be the fact that the *scid* mice have stronger NK-cell activity than wild type mice [27]. To test whether the NK cells played a role in resisting FLV-induced leukemia in the *scid* mice, we generated a *scid* bone marrow transplantation model of FLV-induced leukemogenesis. One week after inoculation with FLV, C3H wild type mice having normal NK activity were transplanted with *scid* bone marrow cells. Even under conditions where host NK-cell activity was not elevated, the transplantation effectively suppressed FLV-induced leukemogenesis as compared with the FLV-inoculated C3H mice transplanted with the wild type C3H bone marrow cells (Fig. 6). Thus, the *scid* mice might be refractory to FLV-induced leukemia not because they have strong NK-cell activity but because the *scid* cells themselves are refractory to viral integration.

3.6. Apoptosis in spleen cells of the FLV-infected scid and ATM −/− mice

The other possibility concerning the resistance of *scid* mice to FLV-induced leukemia would be the increased sensitivity to apoptosis of leukemia cells caused by DNA-PK deficiency. After retroviral infection, integrase-induced DNA breaks are known to cause apoptosis in DNA-PK-deficient *scid* cells in vitro [4]. Therefore, to estimate the apoptotic frequency in FLV-inoculated mice in vivo, spleen cells from wild type, *scid* and *ATM* −/− mice with the C3H background were subjected to the TUNEL assay. As shown in Fig. 7, the apoptotic frequency of spleen cells from the *scid* mice doubled within 12 h after the inoculation with FLV, then gradually

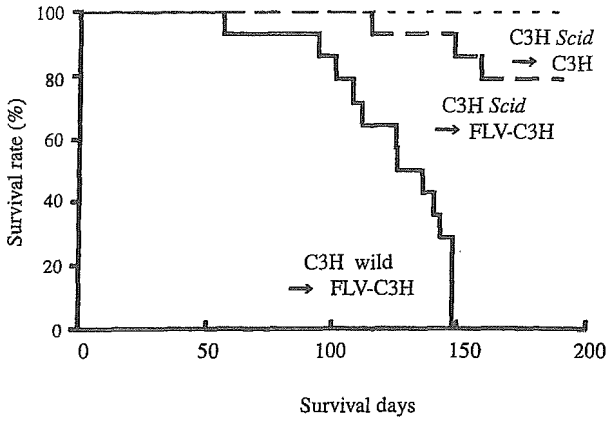

Fig. 6. Effects of *scid* bone marrow transplantation on FLV-infected wild type C3H hosts. Survival curves for C3H wild → FLV-C3H (solid line), C3H *scid* → FLV-C3H (broken line), and C3H *scid* → C3H (dotted line) demonstrating the effects of the *scid* bone marrow cell transplantation on the progression of FLV-induced leukemia. The difference was significant between the *scid* C3H → FLV-C3H and the wild C3H → FLV-C3H mice using Wilcockson's test ($p < 0.01$).

abated, returning to the normal level in 1 week. The apoptotic frequency of spleen cells from the wild type and *ATM* −/− mice did not show significant change after the inoculation. These results indicated that the hematopoietic cells of DNA-PK-deficient *scid* mice might be eliminated by apoptosis after FLV infection in part, however, the apoptotic events occurred only in the early phase of infection and further, the apoptotic cell ratio was not high enough to explain the resistance of *scid* mice to FLV-induced leukemia. Thus, the mechanism of resistance to FLV in *scid* mice appears more complicated than that in the cell culture systems.

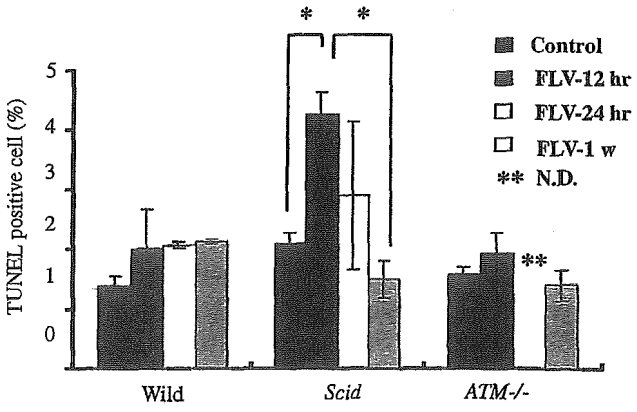

Fig. 7. TUNEL assay for detecting the frequency of apoptotic cells in spleen cells from the wild type, *scid* and *ATM* −/− mice after inoculation with FLV. Bar graphs indicate the mean value of the TUNEL-positive cell ratio (%) of bone marrow in three or four mice from each experimental group. Error bars indicate SEM. Note the remarkable increase of TUNEL-positive cells in the *scid* mice 12 h after FLV inoculation. The difference was significant between the C3H *scid* control and 12 h after FLV inoculation ($p < 0.05$) with Student's *t*-test.

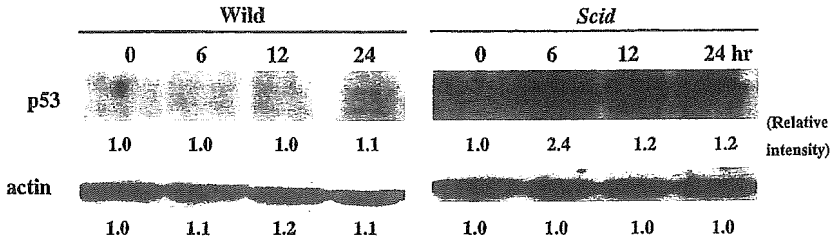

Fig. 8. Western blot analysis for the *p53* status of the FLV-inoculated wild type and *scid* mice after inoculation with FLV. Spleen cells of the wild type and *scid* mice were analyzed for the expression of P53 protein 0, 6, 12 and 24 h after inoculation with FLV. Cells were lysed and whole lysates were examined for P53 expression. The relative intensities of bands were measured by densitometry (0 day, wild type as the control, 1.0) and indicated under the photos of gels. Note the significant increase in P53 expression in the FLV-inoculated *scid* C3H mice in contrast to the almost negative signals in the wild type mice.

3.7. p53 status of the FLV-infected scid mice

p53 is known to regulate multiple cellular functions including cell cycle arrest and apoptosis. To examine whether the *p53* gene was activated in the FLV-inoculated *scid* mice, in other words, to determine whether the apoptosis that occurred in hematopoietic cells of the FLV-inoculated *scid* mice was *p53*-dependent or not, Western blot analysis was performed for P53 protein. Lysates of spleen cells from the wild type and *scid* mice were prepared 6, 12 and 24 h after inoculation with FLV. As shown in Fig. 8, the expression of P53 significantly increased in samples from the *scid* mice compared with wild type mice. Therefore, the *scid* cells might recognize FLV infection as DNA damage and overexpress P53 because of a failure to repair DNA breaks and complete the viral integration process.

4. Discussion

This study clearly demonstrates that DNA-PK-deficient *scid* mice are less susceptible to leukemia and live longer than wild type mice after infection with FLV. In consistent with the in vitro results reported by Daniel et al. [4], *scid* mouse-derived cells were certainly infected with FLV in vivo, although the integration intensity into spleen cells was lower than that in wild type mice. Our experiments revealed that the deficiency for overall integration was about 2–3-fold in *scid* mice, although Daniel et al. showed 5-fold deficiency in the in vitro system. This was consistent with the finding in vitro that DNA-PK was not essential for retroviral integration [9]. However, the most striking events in the viral integration process in *scid* mice was the defective integration of FLV at the *Spi-1* and *Fli-1* sites. As a result, overexpression of these oncogenic transcription factors did not occur in FLV-inoculated *scid* mice. These findings would suggest the significance of DNA-PK for the site-specific integration of retroviral cDNA. However, we have to remember that the defective integration of FLV to these specific sites might be influenced by the lower level of overall random integration in *scid* mice. In contrast, the *ATM* −/− mice exhibited similar changes in leukemogenesis and specific viral integration at the oncogenic transcription factor sites as the wild type mice after inoculation with FLV. These findings are consistent with in vitro data indicating that *ATM* −/− cells were susceptible to retroviral integration [4,28].

A previous study suggests that the abortive integration evoked death in the DNA repair-deficient *scid* cells in vitro [4]. In the present in vivo study also, we showed that apoptosis in hematopoietic cells was more frequent in the *scid* mice than the wild type or *ATM* −/− mice but the difference was not so marked and the change lasted only a short period after the inoculation with FLV. The resistance of *scid* mice to FLV cannot simply be explained by the promotion of apoptosis among retrovirus-infected *scid* cells.

The *ATR* gene [29], may contribute to the end-ligation reaction of DNA at the time of retroviral integration. Usually *ATR* functions in the repair of UV irradiation-induced DNA damage [30], however, we cannot ignore the possibility that this kinase may function under a NHEJ-deficient state. *ATR* overexpression can rescue some of the phenotypes of *ATM* deficiency [31]. The ATR protein phosphorylates a similar set of proteins to ATM, although the kinetics and activation signals involved seem to be different [32]. It seems likely that the specificity of the ATM and ATR reactions is determined by distinct cofactors. Thus, to clarify the function of ATR in vivo, it would be necessary to generate *DNA-PK* and *ATM* double knockout mice as well as *ATR* knockout mice, although this double knockout is known to be fatal [33,34], because the developmental arrest of embryos occurs at around E7.5, a stage when embryonic cells are hypersensitive to DNA damage [35]. Further, the knockout of *ATR* is also embryonic lethal [11].

In terms of immunological protection against FLV-induced leukemia, immunosuppressed animals were expected to be more susceptible to leukemogenesis than the immunocompetent wild type mice [14,36]. In this sense, FLV-induced leukemic cells might proliferate more easily in the immunosuppressed *scid* mice. Actually, FLV-induced disease progressed a little faster in *ATM* −/− mice which also have defects in immunological function [23,24]. Nevertheless, the *scid* mice were rather refractory to FLV-induced leukemogenesis. This may be because specific integration of FLV at the *Fli-1* site no longer occurred and the proliferation of FLV-infected cells in FLV-inoculated *scid* mice was not induced. However, the *scid* mice may have many

other characteristics including loss of mature lymphocytes and high NK-cell activity. As to the target of FLV-induced leukemogensis, the *scid* mice have enough TER119-positive cells in the spleen, although we do not know whether the signal transduction systems of the *scid* erythroid cells are completely the same as the wild type. Further, we cannot ignore the possibility that T cells or B cells might play a role in the integration/proliferation of FLV in the spleen. Although the NK-cell activity did not appear to affect FLV-resistance in the *scid* mice given the results of our BMT experiment, other possibilities should be ruled out to completely clarify the mechanism of resistance in *scid* mice. For example, we could not ignore the possibility that DNA-PK might be necessary for the clonal proliferation of FLV-induced leukemia cells in vivo.

DNA-PK is known to play an important role in the repair of double-stranded DNA breaks including the intermediate state during meiosis and the variable (diversity) joining (V(D)J) recombination by joining broken DNA molecules. However, the mechanisms for specific/non-specific recognition and ligation of blunt ends to form precise joints are still unclear. The joining of retroviral DNA integration has been shown to proceed normally in DNA-PK-deficient cells apart from a small variation in target site duplication. Furthermore, no gross abnormalities in sequence were identified at the provirus–host DNA junctions [37]. Additional experiments will be required to determine the exact role of DNA-PK and associated molecules controlling the specific integration of FLV at the *Spi-1* or *Fli-1* site.

As to the specificity of retroviral integration, the mechanism by which integration sites are chosen is not well understood, and is influenced by several factors, including DNA sequences and structure, DNA methylation and transcription. Viral integrase also plays a key role in controlling the choice of target sites. The integrase domain responsible for target site selection has been mapped to the central core region [38]. Another possible factor directing integration would be the sequence-specific DNA-binding proteins, which may fuse to integrase. Using these fusion proteins, the use of retroviral vectors could be facilitated by targeting integration in vivo at predetermined sites. However, although targeting worked well in reactions in vitro, a variety of obstacles complicated applications in vivo [39]. The present study demonstrated the novel possibility that the host enzyme, DNA-PK, controls the specificity of retroviral integration. We expect the manipulation of host gene function to also be applicable to the design of safer and more effective gene transfer systems in vivo.

Acknowledgements

This work was supported in part by a grant-in-aid for scientific research from the Ministry of Education, Culture, Sports, Science and Technology of Japan. The authors thank Prof. Tom Daniel Humphreys II, Ph.D., University of Hawaii for critical reading of the manuscript with kind and thoughtful suggestions and also for English editing.

Contributions. Maki Hasegawa contributed to the concept and design, interpreted and analyzed the data, provided drafting of the article, provided study materials/patients, and contributed to the collection and assembly of the data. Shuichi Yamaguchi contributed to the concept and design, interpreted and analyzed the data, supplied statistical expertise, and contributed to the collection and assembly of the data. Shiro Aizawa contributed to the concept and design, interpreted and analyzed the data, provided critical revisions and important intellectual content, and obtained a funding source. Hidetoshi Ikeda contributed to the concept and design, interpreted and analyzed the data, provided critical revisions and important intellectual content, and provided study materials/patients. Kouichi Tatsumi interpreted and analyzed the data, provided critical revisions and important intellectual content, and provided study materials/patients. Yuko Noda provided study materials/patients and provided administrative, technical and logistic support. Katsuiku Hirokawa provided critical revisions and important intellectual content, and provided administrative, technical and logistic support. Masanobu Kitagawa contributed to the concept and design, interpreted and analyzed the data, provided drafting of the article, gave final approval, provided study materials/patients, supplied statistical expertise, obtained a funding source, and contributed to the collection and assembly of the data.

References

[1] Katz RA, Skalka AM. The retroviral enzymes. Annu Rev Biochem 1994;63:133–73.
[2] Katz RA, Merkel G, Kulkosky J, Leis J, Skalka AM. The avian retroviral IN protein is both necessary and sufficient for integrative recombination in vitro. Cell 1990;63:87–95.
[3] Craigie R, Fujiwara T, Bushman F. The IN protein of Moloney murine leukemia virus processes the viral DNA ends and accomplishes their integration in vitro. Cell 1990;62:829–37.
[4] Daniel R, Katz RA, Skalka AM. A role for DNA-PK in retroviral DNA integration. Science 1999;284:644–7.
[5] Hartley KO, Gell D, Smith GCM, Zhang H, Divecha N, Connelly MA, et al. DNA-dependent protein kinase catalytic subunit: a relative of phosphatidylinositol 3-kinase and the ataxia telangiectasia gene product. Cell 1995;82:849–56.
[6] Keith CT, Schreiber SL. PIK-related kinases: DNA repair, recombination, and cell cycle checkpoints. Science 1995;270:50–1.
[7] Smith GCM, Jackson SP. The DNA-dependent protein kinase. Genes Dev 1999;13:916–34.
[8] Daniel R, Katz RA, Merkel G, Hittle JC, Yen TJ, Skalka AM. Wortmannin potentiates integrase-mediated killing of lymphocytes and reduces the efficiency of stable transduction by retroviruses. Mol Cell Biol 2001;21:1164–72.
[9] Baekelandt V, Claeys A, Cherepanov P, De Clercq E, De Strooper B, Nuttin B, et al. DNA-dependent protein kinase is not required for efficient lentiviral integration. J Virol 2000;74:11278–85.
[10] Daniel R, Kao G, Taganov K, Greger JG, Favorova O, Merkel G, et al. Evidence that the retroviral DNA integration process triggers an ATR-dependent DNA damage response. Proc Natl Acad Sci USA 2003;100:4778–83.

[11] Cortez D, Guntuku S, Qin J, Elledge SJ. ATR and ATRIP: partners in checkpoint signaling. Science 2001;294:1713–6.
[12] Barlow C, Hirotsune S, Paylor R, Liyanage M, Eckhaus M, Collins F, et al. *Atm*-deficient mice: a paradigm of ataxia telangiectasia. Cell 1996;86:159–71.
[13] Furuno-Fukushi I, Masumura K, Furuse T, Noda Y, Takahagi M, Saito T, et al. Effect of Atm disruption on spontaneously arising and radiation-induced deletion mutations in mouse liver. Radiat Res 2003;160:549–58.
[14] Kitagawa M, Matsubara O, Kasuga T. Dynamics of lymphocytic subpopulations in Friend leukemia virus-induced leukemia. Cancer Res 1986;46:3034–9.
[15] Kitagawa M, Aizawa S, Kamisaku H, Hirokawa K, Ikeda H. Protection of retrovirus-induced disease by transplantation of bone marrow cells transduced with MuLV *env* gene via retrovirus vector. Exp Hematol 1999;27:234–41.
[16] Yamaguchi S, Kitagawa M, Inoue M, Tejima Y, Kimura M, Aizawa S, et al. Role of lymphoid cells in age-related change of susceptibility to Friend leukemia virus-induced leukemia. Mech Ageing Dev 2001;122:219–32.
[17] Paul R, Schuetze S, Kozak SL, Kabat D. A common site for immortalizing proviral integrations in Friend erythroleukemia: molecular cloning and characterization. J Virol 1989;63:4958–61.
[18] Sambrook J, Fritsch EF, Manitais T. Molecular cloning: a laboratory manual. 2nd ed. Cold Spring Harbor, NY: Cold Spring Harbor Laboratory Press; 1989.
[19] Silver J, Kozak C. Common proviral integration region on mouse chromosome 7 in lymphomas and myelogenous leukemias induced by Friend murine leukemia virus. J Virol 1986;57:526–33.
[20] Starck J, Doubeikovski A, Sarrazin S, Gonnet C, Rao G, Skoultchi A, et al. *Spi-1*/PU.1 is a positive regulator of the *Fli-1* gene involved in inhibition of erythroid differentiation in Friend erythroleukemic cell lines. Mol Cell Biol 1999;19:121–35.
[21] Kitagawa M, Takahashi M, Yamaguchi S, Inoue M, Ogawa S, Hirokawa K, et al. Expression of inducible nitric oxide synthase (NOS) in bone marrow cells of myelodysplastic syndromes. Leukemia 1999;13:699–703.
[22] Kitagawa M, Yamaguchi S, Hasegawa M, Tanaka K, Sado T, Hirokawa K, et al. Friend leukemia virus-infection enhances DNA-damage-induced apoptosis of hematopoietic cells in C3H hosts. J Virol 2002;76:7790–8.
[23] Xu Y, Ashley T, Brainerd EE, Bronson RT, Meyn MS, Baltimore D. Targeted disruption of ATM leads to growth retardation, chromosomal fragmentation during meiosis, immune defects, and thymic lymphoma. Genes Dev 1996;10:2383–8.
[24] Chao C, Yang EM, Xu Y. Rescue of defective T cell development and function in *Atm* −/− mice by a functional TCR αβ transgene. J Immunol 2000;164:345–9.
[25] Moreau-Gachelin F, Tavitian A, Tambourin P. *Spi-1* is a putative oncogene in virally induced murine erythroleukaemias. Nature 1988;331:277–80.
[26] Sels FT, Langer S, Schulz AS, Silver J, Sitbon M, Frierich RW. Friend murine leukaemia virus is integrated at a common site in most primary spleen tumours of erythroleukaemic animals. Oncogene 1992;7:643–52.
[27] Christianson SW, Greiner DL, Schweitzer IB, Gott B, Beamer GL, Schweitzer PA, et al. Role of natural killer cells on engraftment of human lymphoid cells and on metastasis of human T-lymphoblastoid leukemia cells in C57BL/6J-*scid* mice and in C57BL/6J-*scid bg* mice. Cell Immunol 1996;171:186–99.
[28] Li L, Olivera JM, Yoden KE, Mitchell RS, Butler SL, Lieber M, et al. Role of the non-homologous DNA end joining pathway in the early steps of retroviral infection. EMBO J 2001;20:3272–81.
[29] Durocher D, Jackson SP. DNA-PK, ATM and ATR as sensors of DNA damage: variations on a theme? Curr Opin Cell Biol 2001;13:225–31.
[30] Shiloh Y. ATM and ATR: networking cellular responses to DNA damage. Curr Opin Genet Dev 2001;11:71–7.
[31] Cliby WA, Roberts CJ, Cimprich KA, Stringer CM, Lamb JR, Schreiber SL, et al. Overexpression of a kinase inactive ATR protein causes sensitivity to DNA damaging agents and defects in cell cycle checkpoints. EMBO J 1998;17:159–69.
[32] Tibbetts RS, Brumbaugh KM, Williams JM, Sarkaria JN, Cliby WA, Shieh SY, et al. A role for ATR in the DNA damage induced phosphorylation of p53. Genes Dev 1999;13:152–7.
[33] Gurley KE, Kemp CJ. Synthetic lethality between mutation in Atm and DNA-PKcs during murine embryogenesis. Curr Biol 2001;11:191–4.
[34] Sekiguchi JA, Ferguson DO, Chen HT, Yang EM, Earle J, Frank K, et al. Genetic interactions between ATM and the nonhomologous end-joining factor in genomic stability and development. Proc Natl Acad Sci USA 2001;98:3243–8.
[35] Heyer BS, MacAuley A, Behrendtsen O, Werb Z. Hypersensitivity to DNA damage leads to increased apoptosis during early mouse development. Genes Dev 2000;14:2072–84.
[36] Zhang F, Ya LT, Iwatani Y, Higo K, Suzuki T, Tanaka M, et al. Resistance to Friend murine leukemia virus infection conferred by the Fv-4 gene is recessive but appears dominant from the effect of the immune system. J Virol 2000;74:6193–7.
[37] Taganov K, Daniel R, Katz RA, Favorova O, Skalka AM. Characterization of retrovirus–host DNA junctions in cells deficient in nonhomologous-end joining. J Virol 2001;75:9549–52.
[38] Holmes-Son ML, Appa RS, Chow SA. Molecular genetics and target site specificity of retroviral integration. Adv Genet 2001;43:33–69.
[39] Bushman FD. Integration site selection by lentiviruses: biology and possible control. Curr Top Microbiol Immunol 2002;261:165–77.